





Doc n°: IA-RP-2000-4122-CNE
Issue: 1.0
Date: 2017-09-27
Sheet: 1 Of: 60

IASI QUARTERLY PERFORMANCE REPORT
FROM 2013/09/01 TO 2013/11/30



BY IASI TEC (TECHNICAL EXPERTISE CENTER)
FOR IASI PFM-R ON METOP B

		Doc n°: IA-RP-2000-4122-CNE Issue: 1.0 Date: 2017-09-27 Sheet: 2 Of: 60
--	---	--

ANALYSE DOCUMENTAIRE

Bordereau d'indexation

Classe (Confidentialité) : NC		Code Consultation :	
Mots clés d'auteur : IASI TEC quarterly synthesis report			
OBJET : <div style="text-align: center;">IASI TEC periodic report</div>			
TITRE : <div style="text-align: center;">IASI quarterly performance report</div>			
Auteur(s) : <div style="text-align: center;">J.Chinaud et Elsa Jacquette (CNES) avec le support de J-C Calvel (AKKA Technologies, marché ACIS 128780)</div>			
RESUME : Quarterly report issued by the IASI TEC team to show trends and layout from the "long term synthesis" TEC function for flags and observables quality indicators			
Document(s) rattaché(s) : Ce document vit seul		Localisation physique du document : Salle IASI TEC	
Volume : <div style="text-align: center;">1</div>	Nombre de pages total : <div style="text-align: center;">60</div> <div style="margin-top: 10px;"> dont - liminaires : 7 annexes : 0 </div>	Nombre d'annexes : <div style="text-align: center;">0</div>	LANGUE : <div style="text-align: center;">English</div>
Document géré en Configuration : <div style="text-align: center;">Non</div>		A DATER DU :	RESPONSABLE :
Contrat : Néant			
SYSTEME HOTE : (logiciel + référence fichier) : <div style="text-align: center;">OpenOffice Writer 3.2</div>			

		Doc n°: IA-RP-2000-4122-CNE Issue: 1.0 Date: 2017-09-27 Sheet: 3 Of: 60
--	---	--

DIFFUSION

On CNES web site : <http://smc.cnes.fr/IASI>
Instrument characteristics / In-orbit performances monitoring

DOCUMENT CHANGE RECORD

Version	Date	Paragraphs	Description
1.0	19/11/13		Creation of the document





		Doc n°: IA-RP-2000-4122-CNE Issue: 1.0 Date: 2017-09-27 Sheet: 4 Of: 60
--	--	--

Table of contents

1 INTRODUCTION.....	8
2 RELATED DOCUMENTS.....	8
2.1 APPLICABLE DOCUMENTS.....	8
2.2 REFERENCE DOCUMENTS.....	8
3 SIGNIFICANT EVENTS.....	9
3.1 EXTERNAL CALIBRATION.....	9
3.2 ON BOARD CONFIGURATION.....	10
3.3 GROUND CONFIGURATIONS UPDATES FOR LEVEL 1 PROCESSING.....	10
3.4 DATA BASES UPDATE FOR THE USERS.....	11
3.5 ON GROUND HW/SW EVOLUTION.....	11
3.6 DECONTAMINATION.....	12
3.7 INSTRUMENT.....	12
3.7.1 External events.....	12
3.7.2 Operation leading to mission outage.....	12
3.7.3 Anomaly leading to mission outage.....	13
4 PERFORMANCE MONITORING.....	14
4.1 PERFORMANCE MONITORING.....	14
4.2 PERFORMANCE SYNOPSIS.....	15
4.3 LEVEL 0 DATA QUALITY (L0).....	16
4.3.1 Overall quality.....	16
4.3.2 Main flag and quality indicator parameters.....	18
4.3.3 Second level flags and quality indicators.....	26
4.3.4 Conclusion.....	26
4.4 LEVEL 1 DATA QUALITY (L1).....	27
4.4.1 Overall quality.....	27
4.4.2 Main flag and quality indicator parameters.....	29
4.4.3 Conclusion.....	33
4.5 SOUNDER RADIOMETRIC PERFORMANCES.....	34
4.5.1 Radiometric Noise.....	34
4.5.2 Radiometric Calibration.....	34
4.5.3 Delay of detection chains.....	39
4.5.4 Optical Transmission.....	40
4.5.5 Interferometric Contrast.....	42
4.5.6 Interferogram Baseline.....	43
4.5.7 Detection Chain.....	44
4.5.8 Conclusion.....	44
4.6 SOUNDER SPECTRAL PERFORMANCES.....	45
4.6.1 Monitoring of the ISRF inputs.....	45
4.6.2 Spectral calibration assessment.....	48
4.6.3 Ghost evolution monitoring.....	50
4.6.4 Conclusion.....	52
4.7 GEOMETRIC PERFORMANCES.....	52
4.7.1 Sounder / IIS co-registration monitoring.....	52
4.7.2 IIS / AVHRR co-registration.....	52

		Doc n°: IA-RP-2000-4122-CNE Issue: 1.0 Date: 2017-09-27 Sheet: 5 Of: 60
--	--	--

4.7.3 Conclusion.....	54
4.8 IIS RADIOMETRIC PERFORMANCES.....	55
4.8.1 IIS Radiometric Noise Monitoring.....	55
4.8.2 IIS Radiometric Calibration Monitoring.....	56
4.8.3 Conclusion.....	58
5 IASI TEC SOFTWARE AND INTERFACES.....	59
5.1 IASI TEC EVOLUTION.....	59
5.2 EUMETCAST INTERFACE.....	59
5.3 FTP INTERFACE.....	59
6 CONCLUSION AND OPERATIONS FORESEEN.....	60
6.1 SUMMARY.....	60
6.2 SHORT-TERM EVENTS.....	60
6.3 OPERATIONS FORESEEN.....	60

Figures and tables

Table 1: External Calibration TEC Requests.....	9
Table 2: DPS and MAS configuration TEC Requests.....	9
Table 3: DPS and MAS previous configuration.....	9
Table 4: IASI L1 Auxiliary File Configuration on the Operational EPS Ground Segment.....	10
Table 5: IASI L1 auxiliary file previous configuration.....	10
Table 6: IASI Data Bases for the users.....	10
Table 7: previous IASI Data Bases.....	10
Table 8: IASI L1 PPF Configuration on the Operational EPS Ground Segment.....	11
Table 9: Previous IASI L1 PPF.....	11
Table 10: Decontamination TEC Requests.....	11
Table 11: Previous decontamination.....	11
Table 12: Overview of METOP manoeuvres in the reporting period.....	11
Table 13: PL-SOL.....	12
Table 14: Scheduled interruptions.....	12
Table 15: Major anomalies.....	12
Table 16: Minor anomalies.....	12
Table 17: Functional status legend	13
Table 18: IASI product components functional status	14
Figure 1 : IASI L0 data quality orbit average (per pixel and CCD).....	15
Figure 2 : IASI L0 data quality spatial distribution (per pixel).....	15
Figure 3 : Temporal evolution of spikes anomaly ratio in % for all pixels (orbit average).....	15
Figure 4 : Geographical distribution of spikes occurrences in % for band 3 and all pixels.....	15
Figure 5 : Temporal evolution of NZPD determination anomaly ratio in % for all pixels (orbit average).....	16
Figure 6 : IASI NZPD determination quality flag spatial distribution (per pixel).....	16
Figure 7 : NZPD inter-pixel for all pixels and CCD calculated with respect to pixel 1 (orbit average).....	16
Figure 8 : IASI L0 over/under-flows orbit average of all pixels.....	17
Figure 9 : IASI Overflows and Underflows spatial distribution (per pixel).....	17
Figure 10 : Max of NZPD quality index for all pixels and CCD - BB.....	17
Figure 11 : Max of NZPD quality index for all pixels and CCD - CS.....	17
Figure 12 : IASI L1 data quality orbit average (% of bad by PN at upper plot and % of good by PN and SB at lower plot).....	18







		Doc n°: IA-RP-2000-4122-CNE Issue: 1.0 Date: 2017-09-27 Sheet: 6 Of: 60
--	--	--

Figure 13 : IASI product overall quality spatial distribution (per pixel).....	18
Figure 14 : GQisQualIndex average (L1 data quality index for IASI sounder).....	18
Figure 15 : GQisQualIndexIIS average (L1 data quality index for IASI Integrated Imager).....	18
Figure 16 : GQisQualIndexSpect average (L1 data index for spectral calibration quality).....	18
Figure 17 : GQisQualIndexRad average (L1 data index for radiometric calibration quality).....	18
Figure 18 : GQisQualIndexLoc average (L1 data index for ground localisation quality).....	19
Figure 19 : MDptPixQual average (L1 quality index for IASI integrated imager, fraction of not dead pixels).....	19
Figure 20 : Instrument noise evolution between start and end of the period.....	19
Figure 21 : Scan mirror reflectivity evolution.....	19
Figure 22 : Radiometric calibration error due to scan mirror reflectivity dependency with viewing angle Maximum effect on SN1 for different scene temperature. Done with the period May / November.....	20
Figure 23 : Black Body Temperature.....	20
Figure 24 : Focal Plane Temperature.....	20
Figure 25 : Monitoring of detection chain maximum delays for all bands.....	20
Figure 26 : Ratio of calibration coefficient slopes as a function of wave number and time after the last decontamination.....	21
Figure 27 : Temporal evolution of calibration ratio coefficient slopes since the last decontamination. The curve was fitted with a decreasing exponential function to determine a rough date for the next decontamination (relative gain evolution of 0.8) ..	21
Figure 28 : Monitoring of contrast for SB3.....	21
Figure 29 : Monitoring of detection chain margins.....	21
Figure 30 : GFaxAxeY average (Y filtered coordinates of sounder interferometric axis).....	23
Figure 31 : GFaxAxeZ average (Z filtered coordinates of sounder interferometric axis).....	23
Figure 32 : Cube Corner offset variation.....	23
Figure 33 : Optical bench Temperature.....	24
Figure 34 : Spectral shift error between L1C IASI and simulated L1C with A4/OP + ECMWF.....	24
Figure 35 : Inter pixel spectral shift error for L1C IASI.....	24
Figure 36 : Ghost amplitude as a function of wave number for different time (Top: pixel 2, bottom: pixel 4).....	25
Figure 37 : Column offset (black) guess vs. column offset averaged over all lines (LN) as a function of the scan position (SP=SN), and orbit number.....	26
Figure 38 : Line offset guess (black) vs. line offset averaged over all lines (LN) as a function of the scan position (SP=SN), and the orbit number.....	26
Figure 39 : Temporal evolution of the noise between start and end of the period.....	26
Figure 40 : Slope and offset coefficients matrix.....	26
Figure 41 : Relative evolution in % of average of slope (red curve) and offset (black curve) coefficients.....	26
Figure 42 : IIS Focal Plane Temperature.....	27
Table 19: IASI TEC at CNES Toulouse.....	28

		Doc n°: IA-RP-2000-4122-CNE Issue: 1.0 Date: 2017-09-27 Sheet: 7 Of: 60
--	---	--

LIST OF ACRONYMS

[TBC]	To be confirmed
[TBD]	To be defined
APO	Other Parameters OPS
AR	Anomaly Report
BRD	BoaRD configuration
CGS	Core Ground Segment at EUMETSAT
CNES	Centre National d'Etudes Spatiales
DA	Applicable document
DPS	Data Processing Subsystem
EPS	EUMETSAT Polar System
EUMETSAT	European organisation for exploitation of METeorological SATellites
FM2 / FM3	Flight Model n°2 or 3
IASI	Infrared Atmospheric Sounding Interferometer
IIS	Integrated Imaging Subsystem
METOP	METeorological OPERational satellite
OPS	Operational Software
PDU	Power Distribution Unit
PL SOL	Payload switch off-line (It's a spacecraft anomaly external to IASI but still resulting in a switch off of the instrument.
PTSI	Parameter Table Status Identifier
RD	Reference document
SEU	Single Event Upset
TEC	IASI Technical Centre of Expertise (located in CNES, Toulouse)
VDS	Verification Data Selection

		Doc n°: IA-RP-2000-4122-CNE Issue: 1.0 Date: 2017-09-27 Sheet: 8 Of: 60
--	---	--

1 INTRODUCTION

The IASI TEC is based at CNES Toulouse and is responsible for the monitoring of the IASI system performances, covering both instrument and level 1 processing sub-system.

This document describes the activities and results obtained at the IASI TEC for instrument PFM-R on METOP-B during the following period:

- Start Time: 2013/09/01 Orbit: 4949
- End Time: 2013/11/30 Orbit: 6241
- Duration: 3 months

Note that IASI ended the Calibration / Validation (commissioning) phase on April 2013.



2 RELATED DOCUMENTS

2.1 *APPLICABLE DOCUMENTS*

N°	Reference	Titre
DA.1	IA-SP-0000-3242-CNE	Spécification de suivi de la performance en vol de IASI sur METOP-A

2.2 *REFERENCE DOCUMENTS*

N°	Reference	Titre

		Doc n°: IA-RP-2000-4122-CNE Issue: 1.0 Date: 2017-09-27 Sheet: 9 Of: 60
--	--	--

3 SIGNIFICANT EVENTS

The following tables present a timeline of the various requests sent by TEC and the external IASI activities.

Those events are typically the configuration changes, programming requests, software update, but also any external operation or activity such as mission interruption, manoeuvre, dissemination problem, ...

3.1 EXTERNAL CALIBRATION

Table 1 shows the External Calibration within the time period reported here. Note that the VDS files that come with each request are not described here.

Execution	TEC ref. ⁽¹⁾	Description	Activities
29/09/2013 from 5h16 to 9h12 orb. 5349 to 5351	RM-06	Monthly_MPF ⁽²⁾ Targets: Earth 15, Blackbody, 2 nd Deep Space, Mirror Backside	For routine monitoring (IIS and IASI NeDT, scan mirror reflectivity, ghost,...)
28/10/2013 from 5h16 to 9h12 orb. 5761 to 5763	RM-07	Monthly_MPF ⁽²⁾ Targets: Earth 15, Blackbody, 2 nd Deep Space, Mirror Backside	For routine monitoring (IIS and IASI NeDT, scan mirror reflectivity, ghost,...)
from 22/11/13 13h22 to 22/11/13 22h20 orb. 6121 to 6126	RL-03	Moon avoidance MPF ⁽²⁾ Targets: 1 st Deep Space	Monitoring of moon intrusion in CS1 FOV
26/11/2013 from 5h16 to 9h12 orb. 6173 to 6175	RM-08	Monthly_MPF ⁽²⁾ Targets: Earth 15, Blackbody, 2 nd Deep Space, Mirror Backside	For routine monitoring (IIS and IASI NeDT, scan mirror reflectivity, ghost,...)

Table 1: External Calibration TEC Requests



⁽¹⁾ TEC convention: R for Routine, M for Monthly and L for moon avoidance, followed by a chronological number

⁽²⁾ An external calibration could be the result of:

- a TEC request or
- a “MPF” uploaded directly by EUMETSAT in full accordance with TEC. The reference “Monthly_MPF” is based on the March 2008 TEC External Calibration request. The MPF for moon avoidance is based on the December 2008 TEC External Calibration request: “ICAL_OCF_xx_M02_20081216060000Z_20090616060000Z_20081209100934Z_IASIT_EXTALIBRA.dts”

Moon external calibration on November 22nd 13:22^Z to 22:20^Z (orbits 6121 to 6126) detail:

External Calibration		External Calibration	
from	to	from	to
2013/11/22 13:22:03	2013/11/22 13:45:15	2013/11/22 18:31:39	2013/11/22 18:55:55
2013/11/22 15:04:59	2013/11/22 15:29:15	2013/11/22 20:15:07	2013/11/22 20:38:19
2013/11/22 16:48:11	2013/11/22 17:12:59	2013/11/22 21:58:35	2013/11/22 22:20:43

		Doc n°: IA-RP-2000-4122-CNE Issue: 1.0 Date: 2017-09-27 Sheet: 10 Of: 60
--	---	---

3.2 ON BOARD CONFIGURATION

Table 2 presents the on-board processing configuration updates that had been made within the time period reported here:

PTSI	IASI on board parameter files	Delivery by TEC	activated on	TEC ref.	affected parameters of a DPS TOP configuration update
10 1.0	IDPS_OBP_xx_M01_20131120160000Z_20140520160000Z_20131120152515Z_IAS_T_DPSPARAMOD.tar	20/11/2013	21/11/2013, orbit 6107	R_37	Update of reduced spectra + modification of BB/CS ZpdQualIndexCutOff

Table 2: DPS and MAS configuration TEC Requests

For information, Table 3 shows the delivery applicable at the beginning of the period:

PTSI	IASI on board parameter files	Delivery by TEC	activated on	TEC ref.	affected parameters of a DPS TOP configuration update
9 1.0	IDPS_OBP_xx_M01_20130704150000Z_20140104150000Z_20130704142055Z_IAS_T_DPSPARAMOD.tar	04/07/2013	10/07/2013, orbit 4203	R_33	Update of reduced spectra Modification of spikes thresholds (2.5e-02) to remove false spikes detection. Modification of ZpdQualIndexCutOff BB/CS (1e-02) to improve on-board filtering. Tuning of IdefSpectrDwn.

Table 3: DPS and MAS previous configuration

The associated ground configuration table (BRD file), necessary to handle coherent configuration at system level, is presented in the next section. These associated configuration table are necessary for L1 processing.

3.3 GROUND CONFIGURATIONS UPDATES FOR LEVEL 1 PROCESSING



Table 4 presents the on-ground processing configuration updates that had been made within the time period reported here:

IDef	IASI L1 auxiliary files	Delivery by TEC	Upload on GS1	Content
37	IASI_BRD_xx_M01_20131120160000Z_XXXXXXZ_20131120152359Z_IAS_T_0000000010	20/11/13	BRD activated on 21/11/2013 13:23, orbit 6107	Linked to PTSI 10
36 18	IASI_BRD_xx_M01_20130905140000Z_XXXXXXZ_20130905121856Z_IAS_T_0000000009 IASI_GRD_xx_M01_20130905140000Z_XXXXXXZ_20130905121902Z_IAS_T_0000000018	15/09/13	BRD&GRD activated on 26/09/2013 12:11, orbit 5311	Modification of IdefIacPosMaxCutoff to be in line with METOP-A processing, update of IDefInterPixNZpd to improve data availability in B1 and B2.

Table 4: IASI L1 Auxiliary File Configuration on the Operational EPS Ground Segment

For information, Table 5 shows the delivery applicable at the beginning of the period:

IDef	IASI L1 auxiliary files	Delivery by TEC	Upload on GS1	Content
33	IASI_BRD_xx_M01_201307150000Z_XXXXXXZ_2013070414174Z_IAS_T_0000000009	04/07/13	BRD activated on 10/07/13 12:59 orbit 4203	Linked to PTSI 9
16	IASI_GRD_xx_M01_20130417100000Z_XXXXXXZ_20130417082744Z_IAS_T_0000000016	17/04/13	GRD activated on 14/05/13 12:05 orbit 3393	Update of scan mirror reflectivity and default values of interferometric axis Update of maximum spectral shift

		Doc n°: IA-RP-2000-4122-CNE Issue: 1.0 Date: 2017-09-27 Sheet: 11 Of: 60
--	---	---

IDef	IASI L1 auxiliary files	Delivery by TEC	Upload on GS1	Content
				(IDefSssWnShiftMax/Min)
12	IASI_ODB_xx_M01_20130417100000Z_XXXXXX XXXXXXZ_20130417082506Z_IAS_0000000012	17/04/13	ODB activated on 14/05/13 12:05 orbit 3393	

Table 5: IASI L1 auxiliary file previous configuration

3.4 DATA BASES UPDATE FOR THE USERS

The Noise Covariance Matrix (NCM) and Spectral data base (SDB) are specific data bases for the users. They are updated according to the main ground level 1 evolutions.

Table 6 presents the updates of the NCM and SDB that had been made within the time period reported here:

IDef	Users Data-Base	Delivery by TEC	TEC ref.	Comments
12	IASI_SDB_xx_M01_20130923150000Z_2 0130923150000Z_20130923132439Z_IAS T_IASISPECDB	25/09/13	R_33	User database associated to ODB IDefSDB 12

Table 6: IASI Data Bases for the users

For information, Table 7 shows the delivery applicable at the beginning of the period:

IDef	Users Data-Base	Delivery by TEC	TEC ref.	Comments
2	IASI_NCM_xx_M01_20130522081244Z_2 20130522081244Z_20130522081245Z_IA ST_SPECTRESPO	22/05/13	CVA_COV_2	Update of NCM
10	IASI_SDB_xx_M01_20130315083000Z_2 0130315083000Z_20130315082843Z_IAS T_IASISPECDB	15/03/13	CVB_23	User database associated to ODB IDefSDB 10

Table 7: previous IASI Data Bases

3.5 ON GROUND HW/SW EVOLUTION

Table 8 presents the updates of PPF L1 software within the time period reported here:



IASI L1 PPF software version	Delivery by TEC	Date introduced on GS1	Comments

Table 8: IASI L1 PPF Configuration on the Operational EPS Ground Segment

For information, Table 9 shows the software version applicable at the beginning of the period:

IASI L1 PPF software version	Delivery by TEC	Date introduced on GS1	Comments
7.0	07/2013	08/08/2013 for sensing time 08:11 ^{UTC} Orbit 35299	

Table 9: Previous IASI L1 PPF

		Doc n°: IA-RP-2000-4122-CNE Issue: 1.0 Date: 2017-09-27 Sheet: 12 Of: 60
--	---	---

3.6 DECONTAMINATION

Table 10 presents decontaminations that have been made or requested within the time period reported here:

Last due date	Date of decontamination	Description
March 2014		

Table 10: Decontamination TEC Requests

For information, Table 11 shows the previous decontamination:

Last due date	Date of decontamination	Description

Table 11: Previous decontamination

3.7 INSTRUMENT

3.7.1 External events

This category is for those activities/events that are external to IASI but still have an impact. It is broken down into classes of PL-SOL and OOP manoeuvre.

3.7.1.1 Manoeuvres

Date	Type ^(*)	Description	IP flag	OoP mission Outage
05/11/2013	OoP	OoP manoeuvre #7		From 8:12 to 14:24

Table 12: Overview of METOP manoeuvres in the reporting period

(*): IP for In-Plane manoeuvres (IASI stays in NOP) and OoP for Out of plane manoeuvres (IASI is put in Heater 2)

3.7.1.2 PL-SOL

Table 13 presents the PL-SOL events that have occurred within the time period reported here:

Dates	Orbits	Description
2013/10/16 11:49 to 11:58	5593-5594	IIS Equalization
2013/10/29 06:26 to 10:51	5777-5779	ANO PLM SSR : Payload anomaly : SSR in wait mode. Loss of data (science+HK) during 4:20 hours



Table 13: PL-SOL

3.7.2 Operation leading to mission outage

This chapter presents the intervention on IASI needing routine interruption that have occurred within the time period reported here.

Dates	Orbits	type	IASI mode	Description

Table 14: Scheduled interruptions

		Doc n°: IA-RP-2000-4122-CNE Issue: 1.0 Date: 2017-09-27 Sheet: 13 Of: 60
--	--	---

3.7.3 Anomaly leading to mission outage

Table 15 and Table 16 present the major and minor anomalies internal to IASI that have occurred within the time period reported here.

Note that, in this section minor anomalies are all identified and without any impact on the mission, and major anomalies only affect IASI instrument, and no other sub-systems of the spacecraft.



Dates	Orbits	Anomaly type (*)	IASI mode	Description

Table 15: Major anomalies

(*): SEU (LAS, CCM or DPS) anomalies or SET anomalies

Day	Orbits	error n°	Severity	Anomaly type	LN	SN	Description
2013/11/25 22:46:29	5077			CCM - CSQ	32595	33	minor anomaly BW lat 8.5°S, lon: 17.4°W

Table 16: Minor anomalies

		Doc n°: IA-RP-2000-4122-CNE Issue: 1.0 Date: 2017-09-27 Sheet: 14 Of: 60
--	---	---

4 PERFORMANCE MONITORING

4.1 *PERFORMANCE MONITORING*

In order to ensure that the IASI system is permanently running in good conditions, the CNES (IASI TEC) and EUMETSAT (CGS) are monitoring each orbit, both at line, PDU and DUMP levels.



The on-board and ground processing performance algorithms issue more than one hundred quality indicators, called flags and simple parameters. Those are alarms for any bad functioning or local performance degradation.

According to the results, the TEC is also in charge of delivering new on-board or ground parameters to EUMETSAT when it is necessary. EUMETSAT is then in charge of uploading them on-board or as an input of the level 1 processing chain. During the whole instrument life, these parameter adjustments are necessary in order to take into account instrument evolution in the processing and finally to maintain a good data quality.

The Table 17 is the colour code used for the status report.

Status Colour	Meaning
GREEN	≥ 95
YELLOW	< 95
RED	Production interrupted
BLANK	No Status Reported

Table 17: Functional status legend



		Doc n°: IA-RP-2000-4122-CNE Issue: 1.0 Date: 2017-09-27 Sheet: 15 Of: 60
--	---	---

4.2 PERFORMANCE SYNOPSIS

Table 18 provides a synthetic view of all the indicators evaluated for L0/L1 data and their current status.

Section	Component	Description	Status	Comments
4.3	L0	Level-0 Data Quality <ul style="list-style-type: none"> Overall quality Main flag and quality indicator parameters <ul style="list-style-type: none"> Spikes monitoring ZPD monitoring Overflows/Underflows monitoring Reduced Spectra monitoring Second level flag and quality indicators 	GREEN	On-board processing
4.4	L1	Level-1 Data Quality <ul style="list-style-type: none"> Overall Main flag and quality indicator parameters Second level flag and quality indicators 	GREEN	On ground processing
4.5	L1	Sounder radiometric performances <ul style="list-style-type: none"> Radiometric noise Radiometric calibration Optical transmission Interferometric contrast Detection chain 	GREEN	
4.6	L1	Sounder spectral performances <ul style="list-style-type: none"> Dimensional stability Acquisition chain delay Ghost evolution Instrument parameters 	GREEN	
4.7	L1	Geometric performances <ul style="list-style-type: none"> Sounder/IIS co-registration IIS/AVHRR co registration 	GREEN	
4.8	L1	IIS radiometric performances <ul style="list-style-type: none"> IIS radiometric noise monitoring IIS radiometric calibration monitoring 	GREEN	

Table 18: IASI product components functional status

		Doc n°: IA-RP-2000-4122-CNE Issue: 1.0 Date: 2017-09-27 Sheet: 16 Of: 60
--	---	---

4.3 LEVEL 0 DATA QUALITY (L0)

4.3.1 Overall quality

The IASI L0 data quality (orbit average) through IASI engineering products is shown in Figure 1.

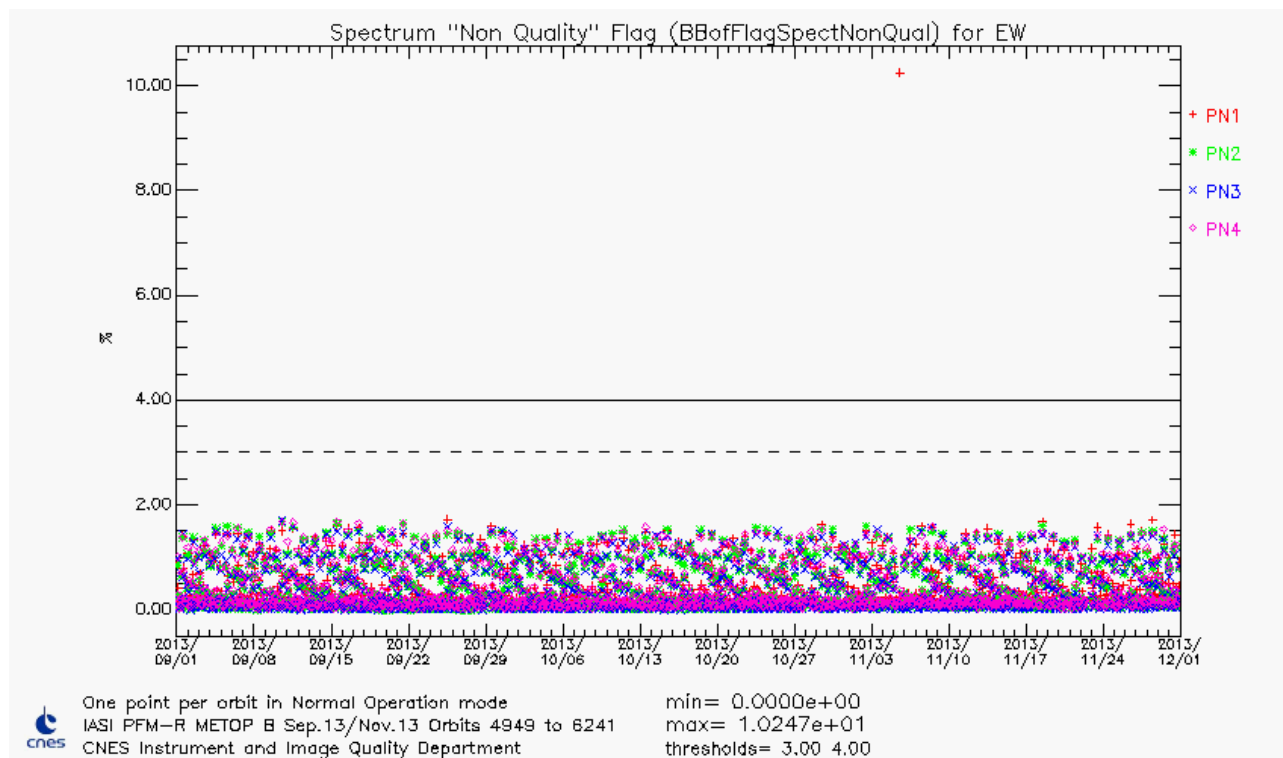


Figure 1 : IASI L0 data quality orbit average (per pixel and CCD)

The peak observed in November is due to an anomaly that occurred after an out of plane manoeuvre where IASI on MetOp-B was on Heater 2 mode. When IASI went back to normal operation at 14:24 UTC, the data quality was degraded on several pixels until 15:44 UTC : This was due to a need of reduced spectra update, see 4.3.2.4. for more explanation.

The geographical distribution of the overall L0 (board) quality flag for the 4 pixels is shown in Figure 2.



Doc n°: IA-RP-2000-4122-CNE

Issue: 1.0

Date: 2017-09-27

Sheet: 17 Of: 60

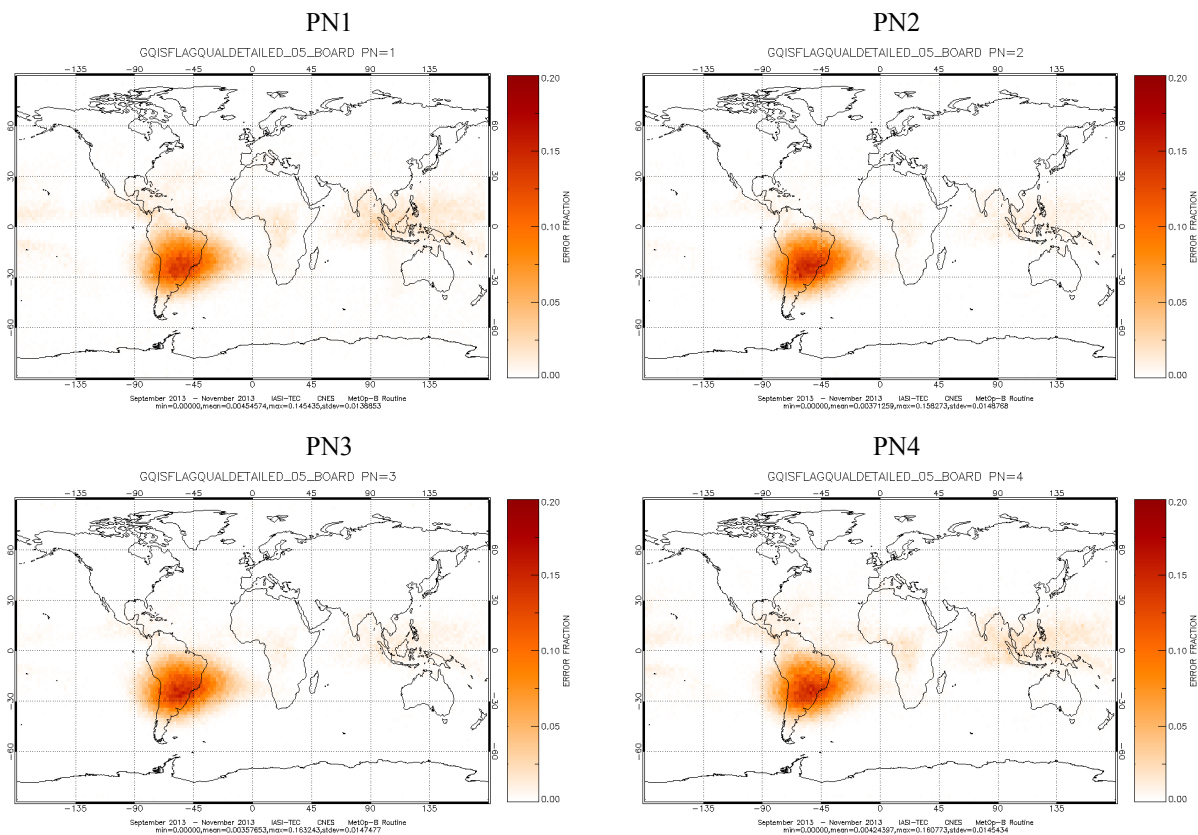




Figure 2 : IASI L0 data quality spatial distribution (per pixel)

The IASI L0 quality and on-board processing are nominal.

		Doc n°: IA-RP-2000-4122-CNE Issue: 1.0 Date: 2017-09-27 Sheet: 18 Of: 60
--	--	---

4.3.2 Main flag and quality indicator parameters

The main contributors to the rejected spectra by on-board processing are: the spikes (proton interaction on detectors), failure of NZPD algorithm determination and over/underflows (measured data exceeding on-board coding tables capacity). They are analysed in details hereafter.

4.3.2.1 Spikes monitoring

Spikes occur when a proton hits a detector. This very high energetic particle disrupts the measure of the interferogram and then corrupts the spectrum.

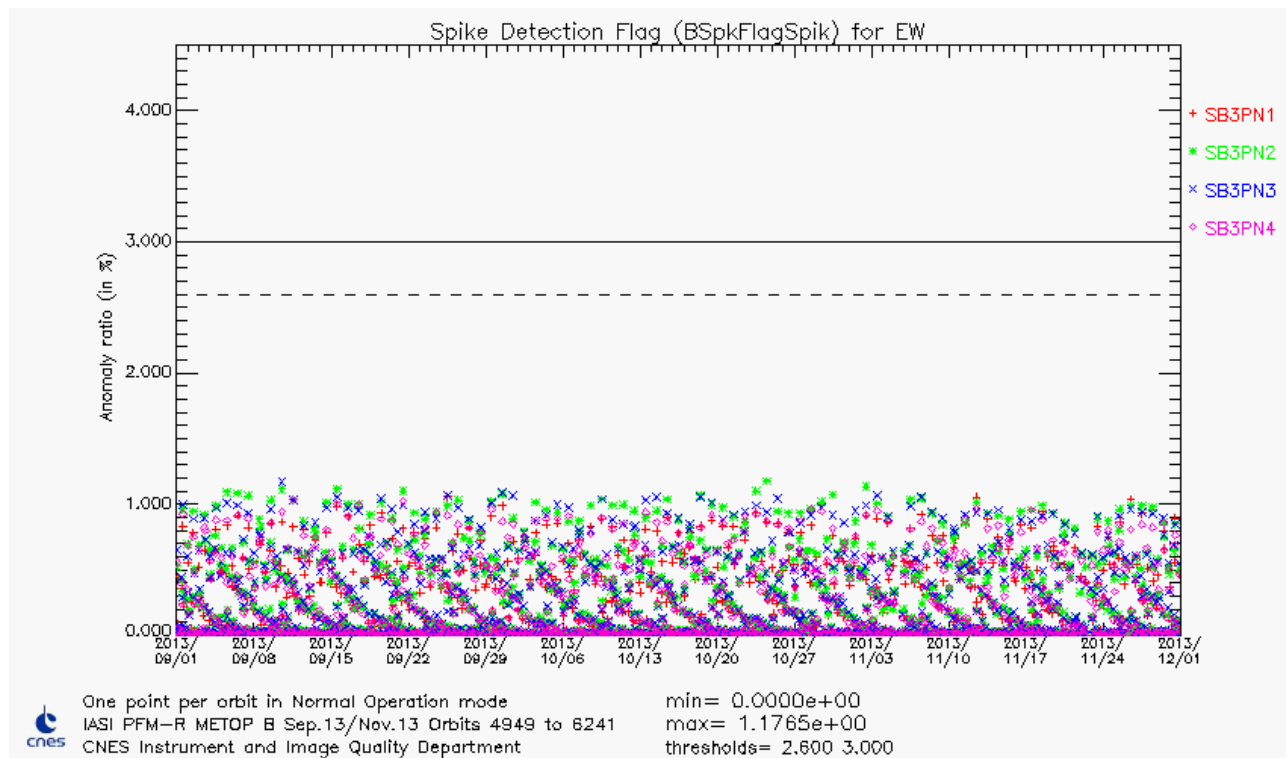


Figure 3 : Temporal evolution of spikes anomaly ratio in % for all pixels (orbit average)

An example of the geographical distribution of spikes occurrences on band 3 for the 4 pixels is shown in Figure 4.



Doc n°: IA-RP-2000-4122-CNE

Issue: 1.0

Date: 2017-09-27

Sheet: 19 Of: 60

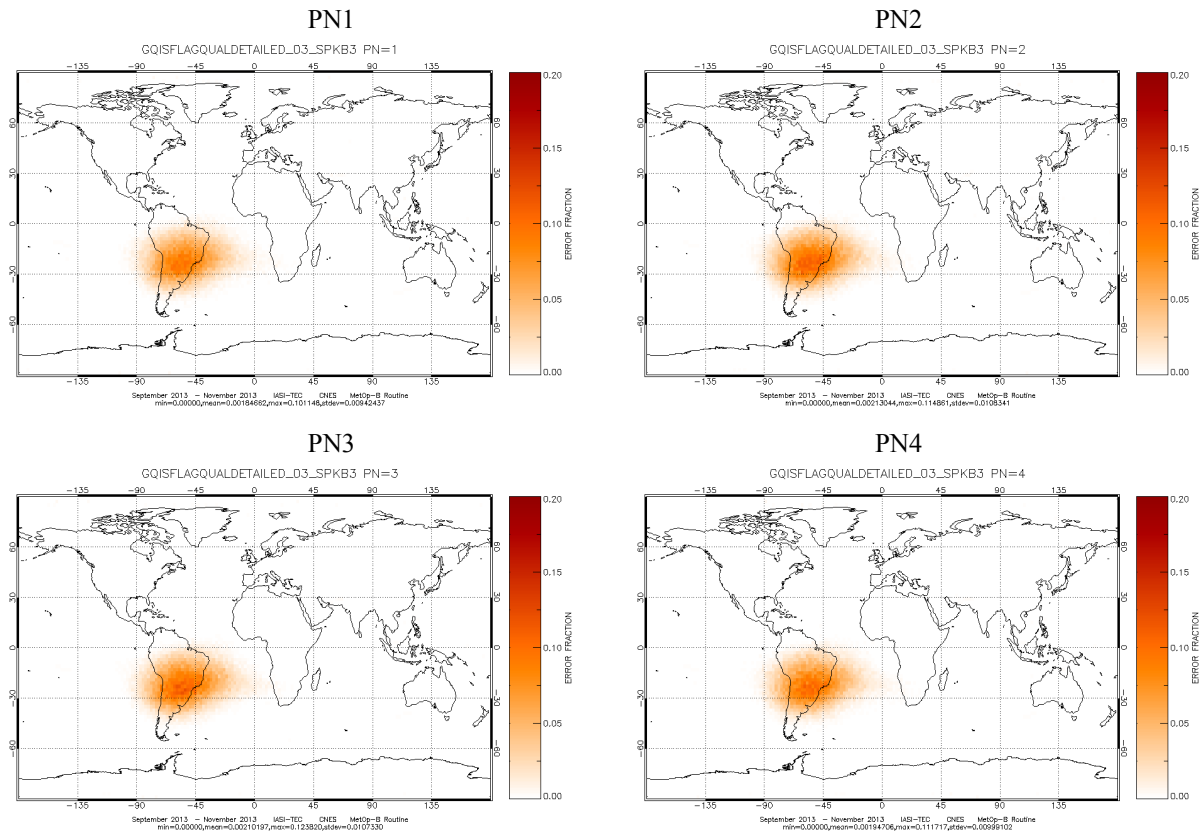




Figure 4 : Geographical distribution of spikes occurrences in % for band 3 and all pixels

Spikes are mainly located in the regions of Earth where the magnetic field doesn't protect the satellite from the energetic particles : the poles and the SAA (South Atlantic anomaly).

Spike anomaly ratio is nominal for the reported period.

		Doc n°: IA-RP-2000-4122-CNE Issue: 1.0 Date: 2017-09-27 Sheet: 20 Of: 60
--	--	---

4.3.2.2 ZPD monitoring

The ZPD (“Zero Path Difference”) is the position of the central fringe of the interferogram. The NZPD is the number of the sample detected as the ZPD. On IASI, it is determined by a software. This is a special feature of IASI in comparison to other instruments for which NZPD determination is done by hardware.

NZPD variations are governed by two phenomenons:

1. ASE fluctuations which have the same effect on each pixel and can produce NZPD variation of 30-40 samples over month. This is the first order phenomena.
2. Mechanical deformation of the interferometer or evolution of detection chain delays. These phenomenons affect the 4 pixels in different way. However this phenomenon has a second order effect in comparison to the first one.

We monitor both NZPD determination quality flag and interpixel homogeneity. We expect a stability.

BZPDFlagNZPDNonQualEW: Temporal evolution of NZPD determination quality flag for earth view

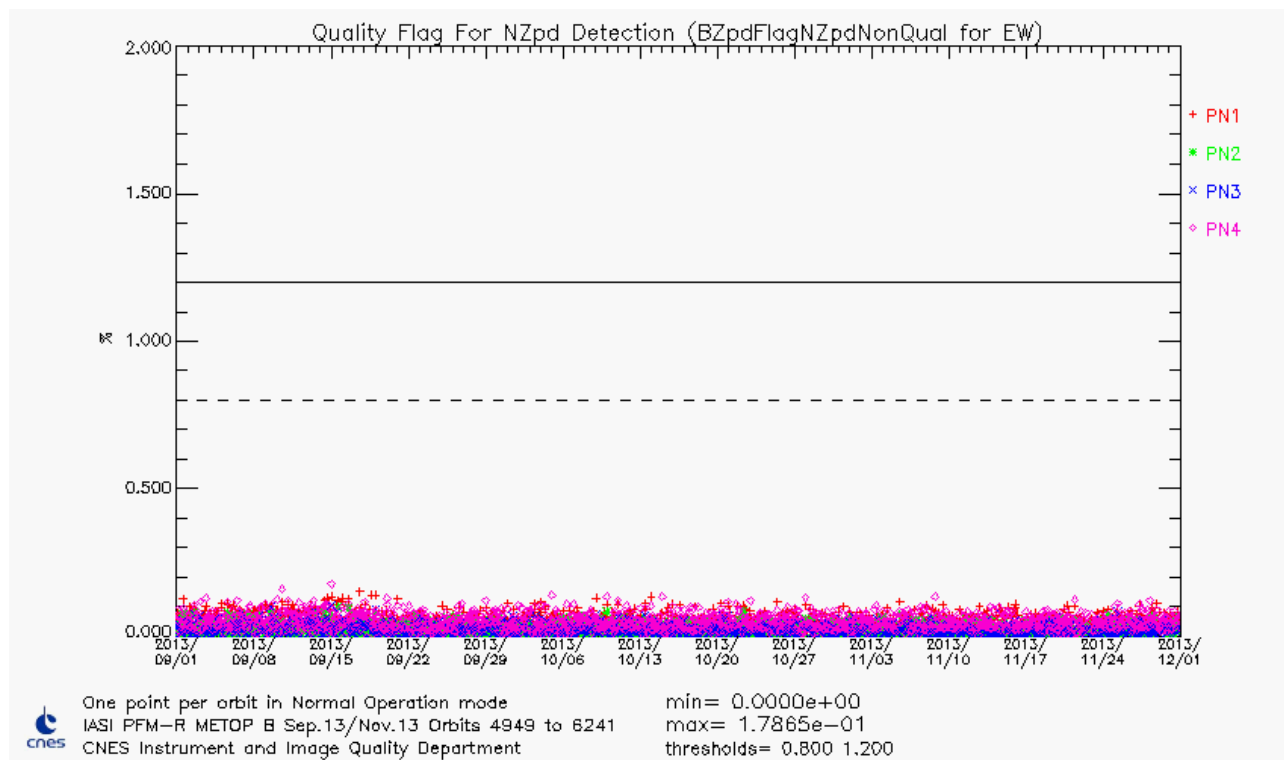


Figure 5 : Temporal evolution of NZPD determination anomaly ratio in % for all pixels (orbit average)

NZPD determination anomaly ratio is nominal for the reported period.

The geographical distribution of the NZPD determination quality flag for the 4 pixels is shown in Figure 6.

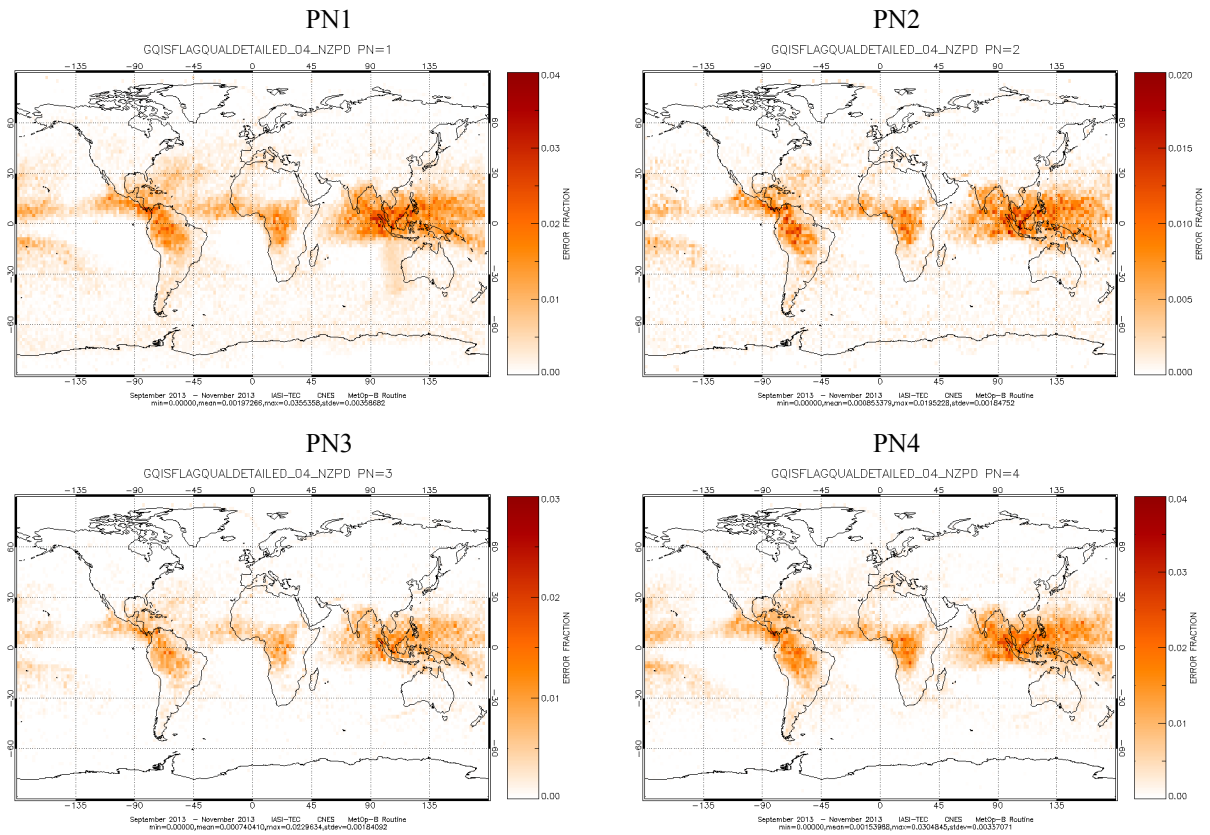




Figure 6 : IASI NZPD determination quality flag spatial distribution (per pixel)

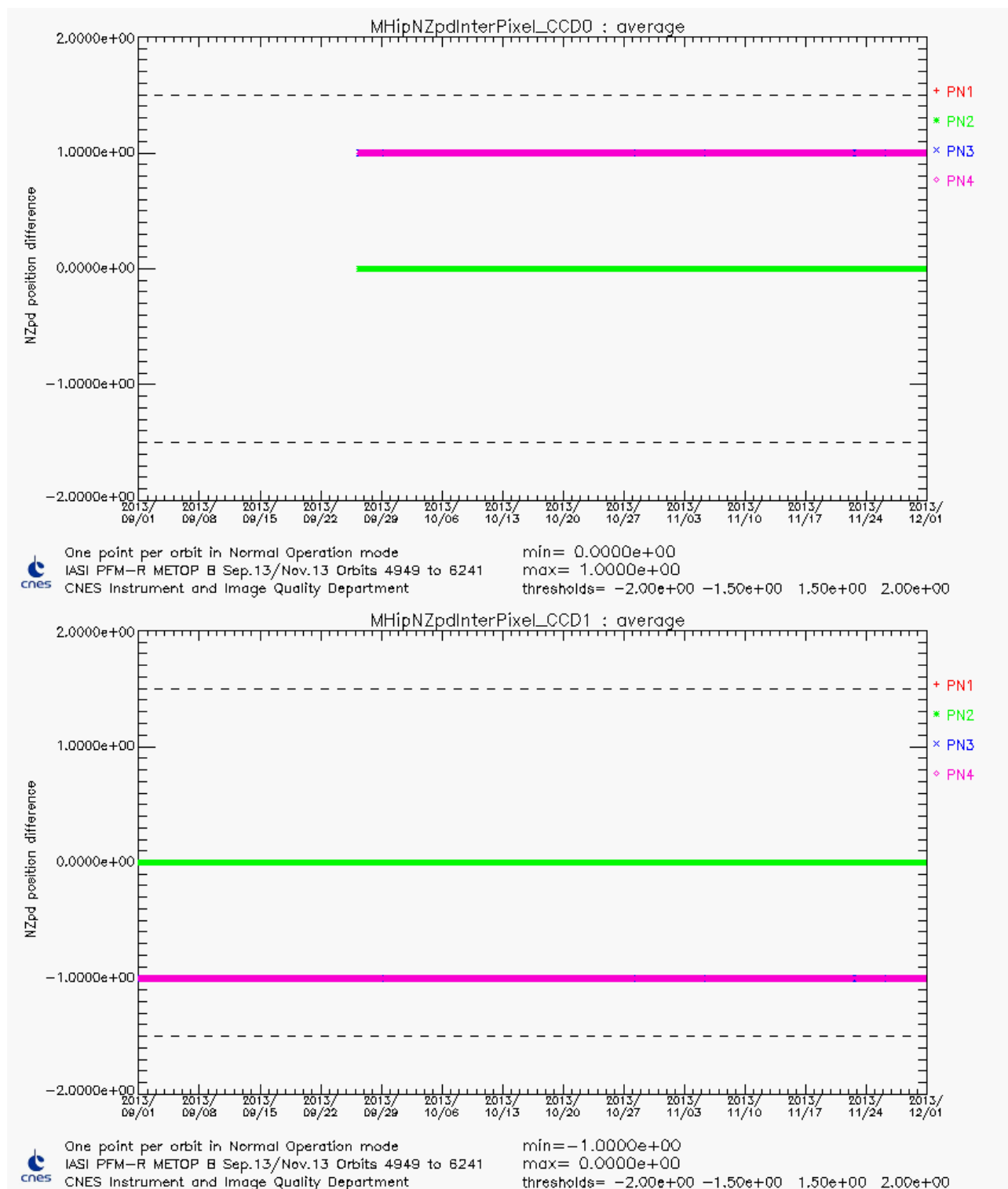
The NZPD determination fails over some clouds that have a temperature that induces no energy in the central fringe of the interferogram.

		Doc n°: IA-RP-2000-4122-CNE Issue: 1.0 Date: 2017-09-27 Sheet: 22 Of: 60
--	--	---

NZPD inter-pixel homogeneity monitoring

This monitoring is necessary in order to follow potential deformation of the interferometer or evolution of detection chain delay.

Between the upload of TOP PTSI 9 on 10/07/2013 and the update of on-ground configuration BRD 36 on 26/09/2013, the NZPD inter-pixel calculated on-board for CCD0 is not in line with the content of the ground configuration (parameter IdefInterpixNZPD). Consequently, the L1 processing can not perform spectrum rescue in B1 and B2. In case of spikes in B3 for CCD0 (which means a loss of ~0.1 % of spectra in B1 and B2). This problem was solved by the update of the ground configuration in September.





		Doc n°: IA-RP-2000-4122-CNE Issue: 1.0 Date: 2017-09-27 Sheet: 23 Of: 60
--	--	---

Figure 7 : NZPD inter-pixel for all pixels and CCD calculated with respect to pixel 1 (orbit average)

4.3.2.3 Overflows / Underflows monitoring

The total number of bits available for a spectrum to be transmitted to the ground is limited. For that reason, we have defined coding tables to encode each measured spectrum. These tables have been design by using “extreme spectrum” corresponding to known drastic atmospheric conditions. The coding step is also set to not introduce additional noise into the spectrum. However for very extreme atmospheric conditions (sunglint in B3, very high stratospheric temperature...) a measure can exceed on-board coding tables’ capacity and causes an over/underflow.

Over/underflows occurrences are monitored and stability is expected. As long as they remain to low levels, the coding table is not changed. Note that changing the coding tables requires compromises. Indeed, increasing the encoding capacity can be achieved by two different ways. A first solution consists in an increase of the coding step without changing the number of bits. However, that leads to an increase of the digitalization noise. Then, a second solution consists in keeping the coding step constant while increasing the number of bits available for a particular band. But, the total amount of bits available for the entire spectrum is limited and constant. So, that requires to decrease the encoding capacity in another spectral band.

Time series of Overflows and Underflows (orbit average) are shown in following figure for all pixels.

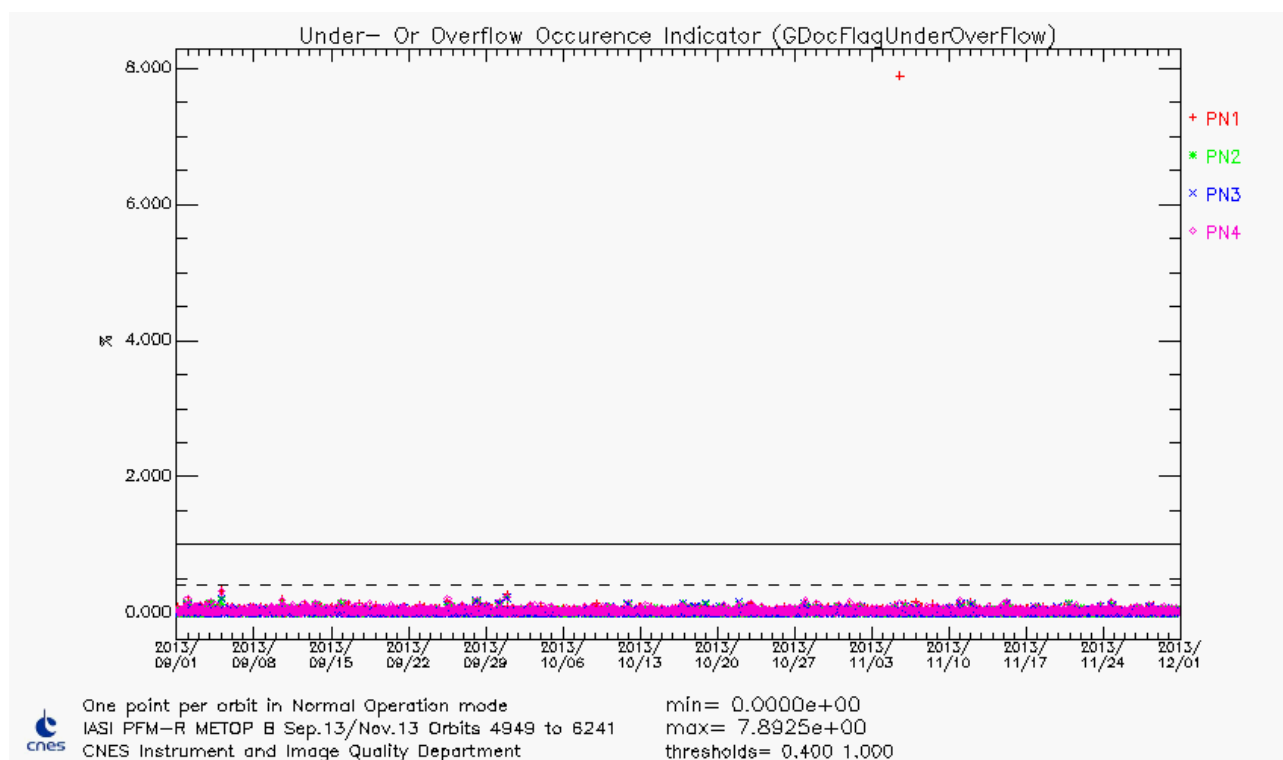


Figure 8 : IASI L0 over/under-flows orbit average of all pixels

Over/underflows ratio is nominal for the reported period. (see 4.3.1 for peak observed on 05/11/2013)

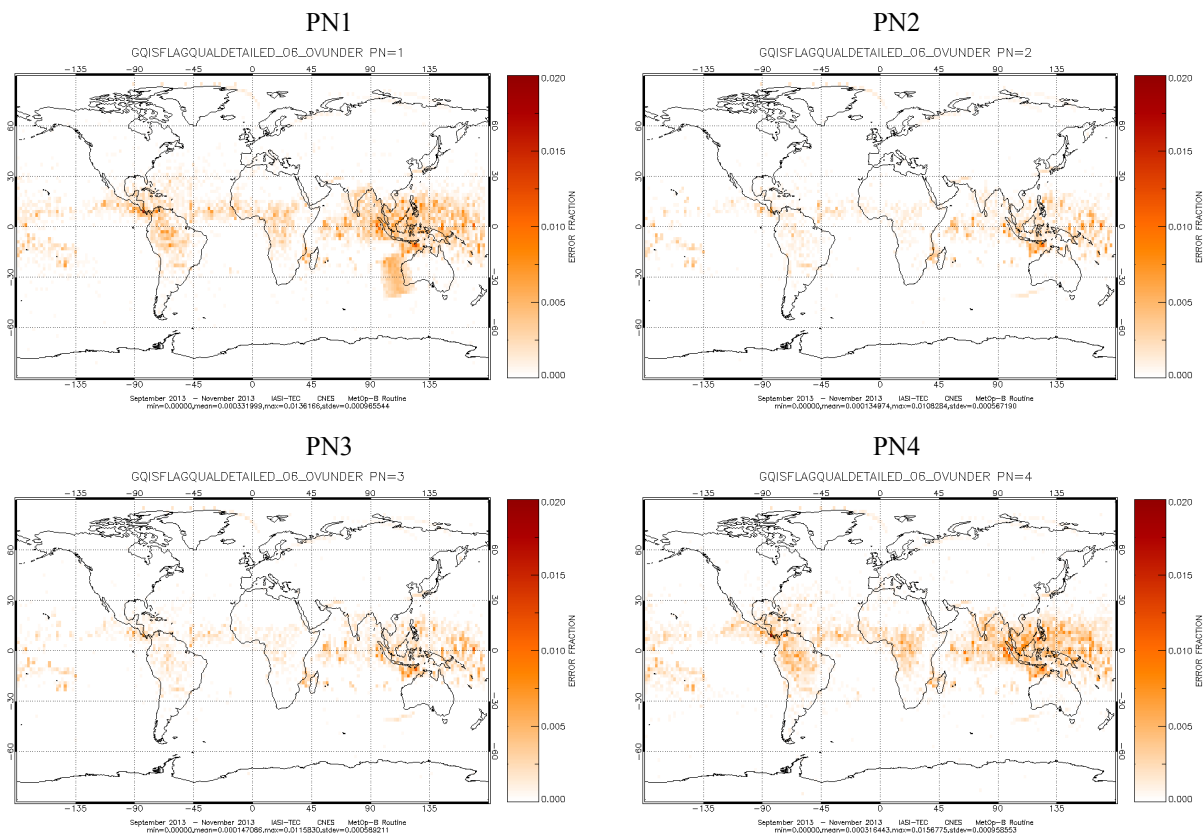


Figure 9 : IASI Overflows and Underflows spatial distribution (per pixel)

4.3.2.4 Reduced Spectra monitoring

On-board Reduced Spectra is one of the most important monitoring. It ensures that on-board spectra still have a good radiometric calibration when on-board configuration reduced spectra are reloaded. This is the case, for instance, after an instrument mode change.

Reduced spectra are slightly evolving with respect to potential deformation of the interferometer (optical bench).

In order to prevent a large difference between current and on-board configuration reduced spectra, we monitor the evolution of ZPD determination quality index for calibration views (BZpdNzpdQualIndexBB and CS) obtained by DPS processing by simulating a perpetual mode change. Results of this monitoring are given hereafter.

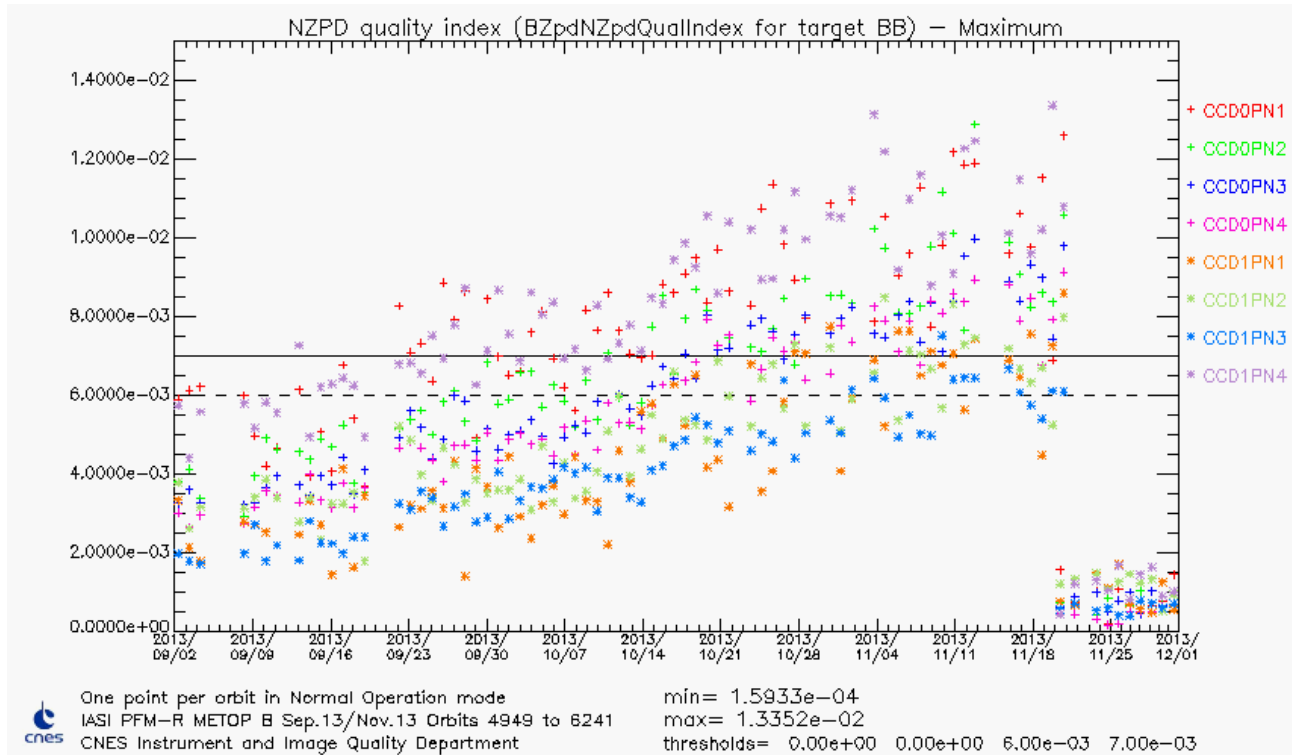


Figure 10 : Max of NZPD quality index for all pixels and CCD - BB

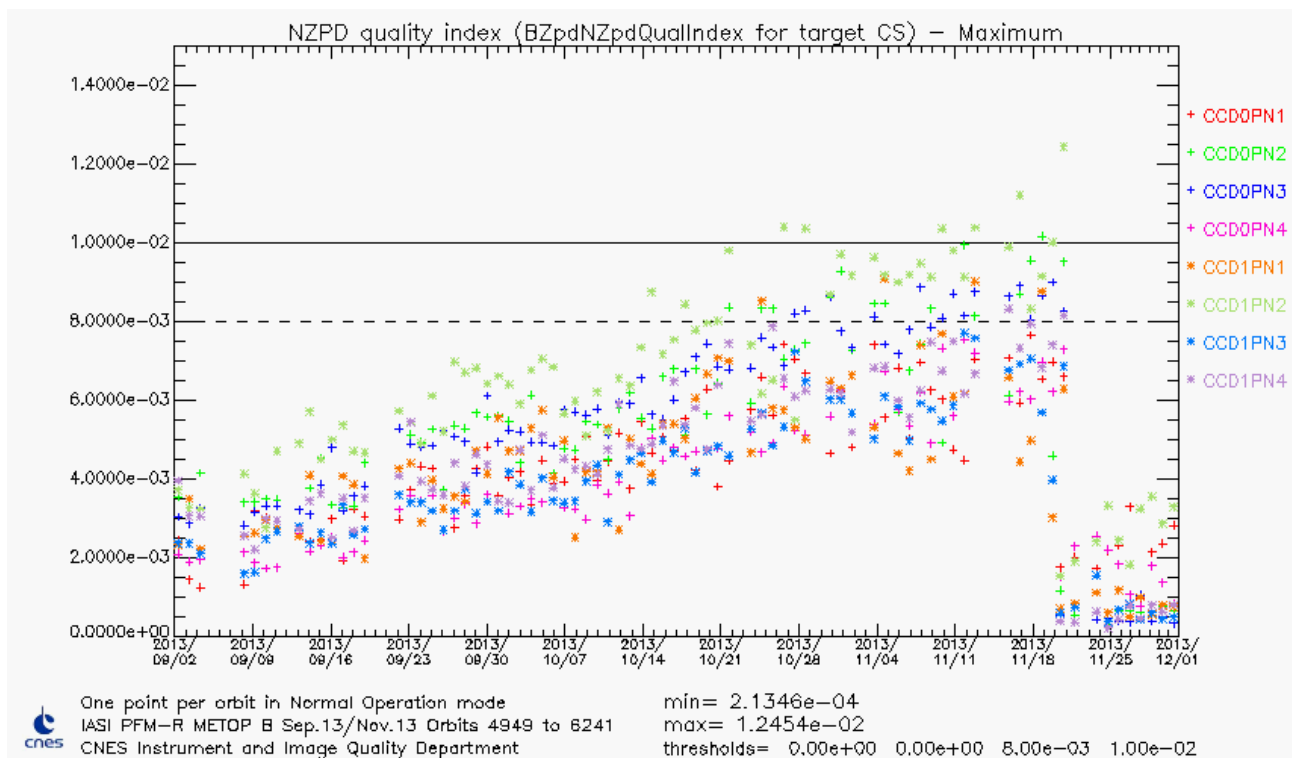




Figure 11 : Max of NZPD quality index for all pixels and CCD - CS

As soon as BZPDNZPDQualIndexBB and CS remain below 0.02 on-board reduced spectra are robust to an instrument mode change.

The reduced spectra quality is well within specification since the last update of the on-board reduced spectra performed in November 2013.

		Doc n°: IA-RP-2000-4122-CNE Issue: 1.0 Date: 2017-09-27 Sheet: 26 Of: 60
--	---	---

4.3.3 Second level flags and quality indicators

All second level flags and indicators are stable and nominal.



4.3.4 Conclusion

On PTSI 9 (from 10/07/2013 to 21/11/2013), the BB/CS ZpdQualIndexCutOff was set to 0.01 (instead of 0.02) to avoid to take into account bad measurements in the reduced spectra (due to an anomaly on 23/04/2013). So, when an instrument mode change occur, on-board reduced spectra are robust only if BZPDNZPDQualIndexBB and CS are under 0.01. This threshold was reached on october 2013.

IASI was on heater 2 mode during the out of plane manoeuvre on 05/11/2013, when it comes back to normal operation, it loads the reduced spectra of the configuration, but they were not up to date. Indeed, in the first year of its life, the IASI instrument characteristics evolves a bit, in particular the NZpd location in the interferograms, mainly due to desorption and mechanical small deformations. The reduced spectra of the current configuration were a bit too far from the current state of the instrument, and the threshold on NZpdQualIndex of calibration views prevents the use of the current calibration views to compute the NZpd, leading to a bad determination of NZpd on board, and thus to unusable spectra. It leads to a degraded quality of the data during 1:20 hours on 05/11/2013.

New reduced spectra were computed, the on-board configuration file was loaded in operation on 21/11/2013. In PTSI 10, the BB/CS ZpdQualIndexCutOff was set back to 0.02.

Since this last update, the reduced spectra quality is good.

		Doc n°: IA-RP-2000-4122-CNE Issue: 1.0 Date: 2017-09-27 Sheet: 27 Of: 60
--	--	---

4.4 LEVEL 1 DATA QUALITY (L1)

4.4.1 Overall quality

The IASI overall quality is shown as the orbit averages of the quality indicator for the individual pixels in the next figure.

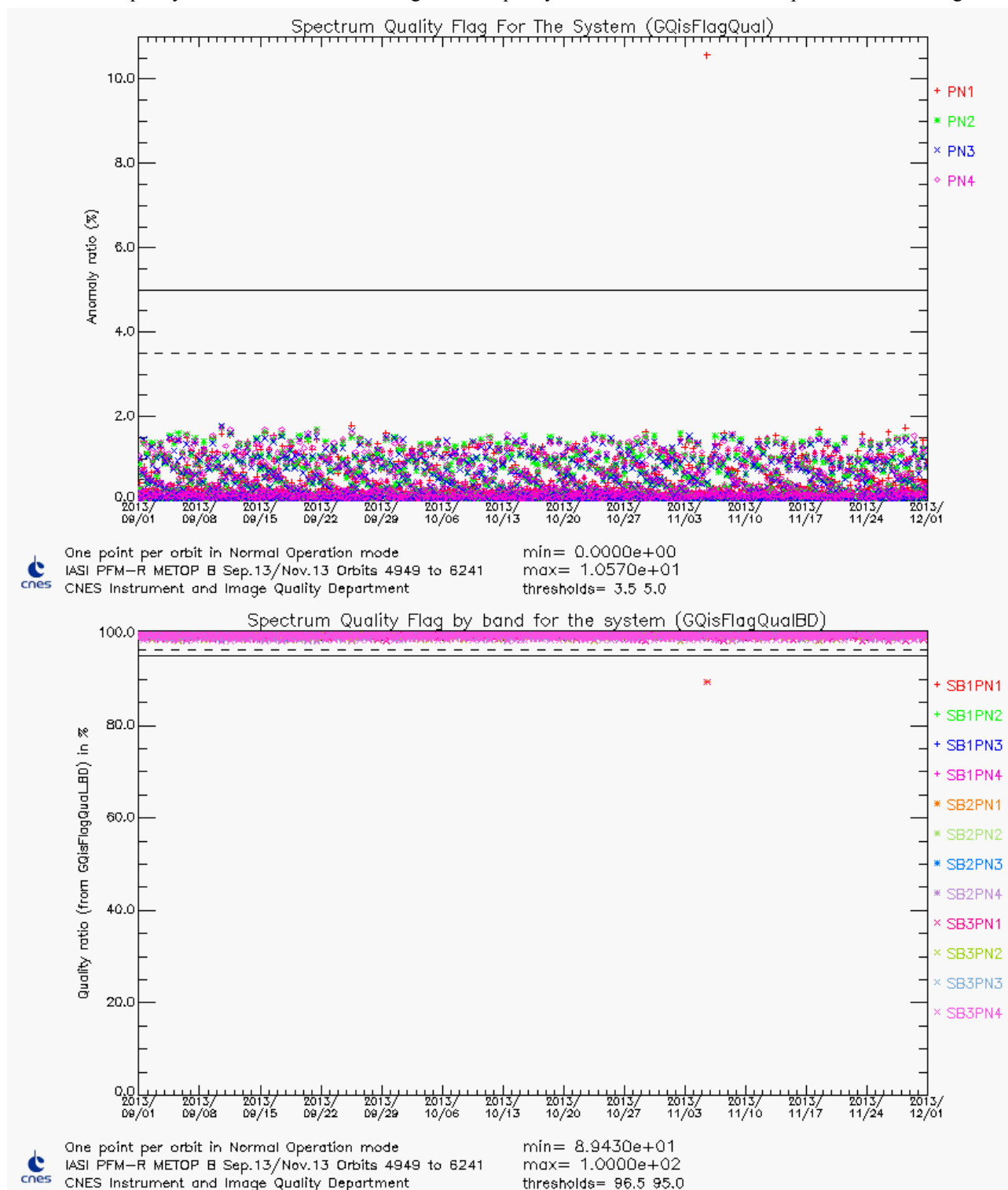




Figure 12 : IASI L1 data quality orbit average (% of bad by PN at upper plot and % of good by PN and SB at lower plot)

One should note that, over the period covered by the present document, the averaged data rejection ratio is less than 1%. (see 4.3.1 for peak observed on 05/11/2013)

		Doc n°: IA-RP-2000-4122-CNE Issue: 1.0 Date: 2017-09-27 Sheet: 28 Of: 60
--	--	---

The geographical distribution of the IASI product overall quality for the 4 pixels is shown in Figure 13.

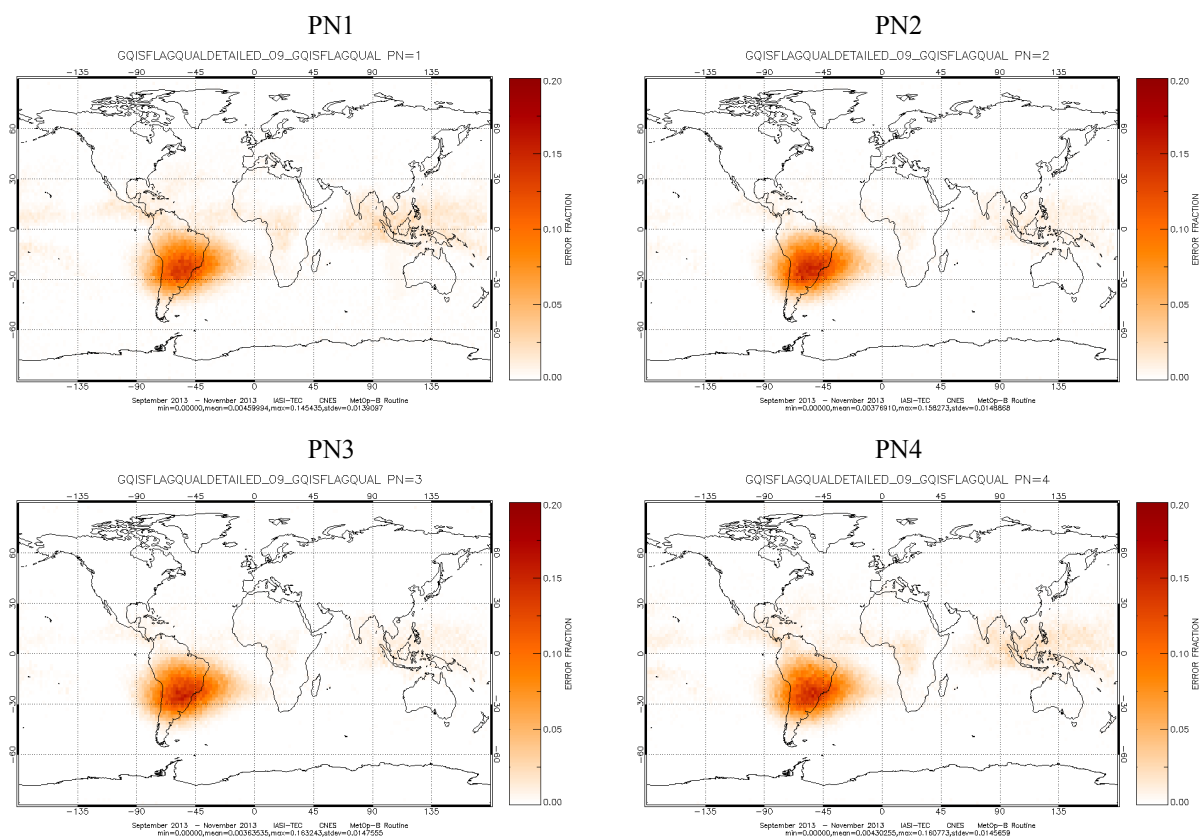




Figure 13 : IASI product overall quality spatial distribution (per pixel)

The main contributors are the spikes in band 3.

		Doc n°: IA-RP-2000-4122-CNE Issue: 1.0 Date: 2017-09-27 Sheet: 29 Of: 60
--	--	---

4.4.2 Main flag and quality indicator parameters

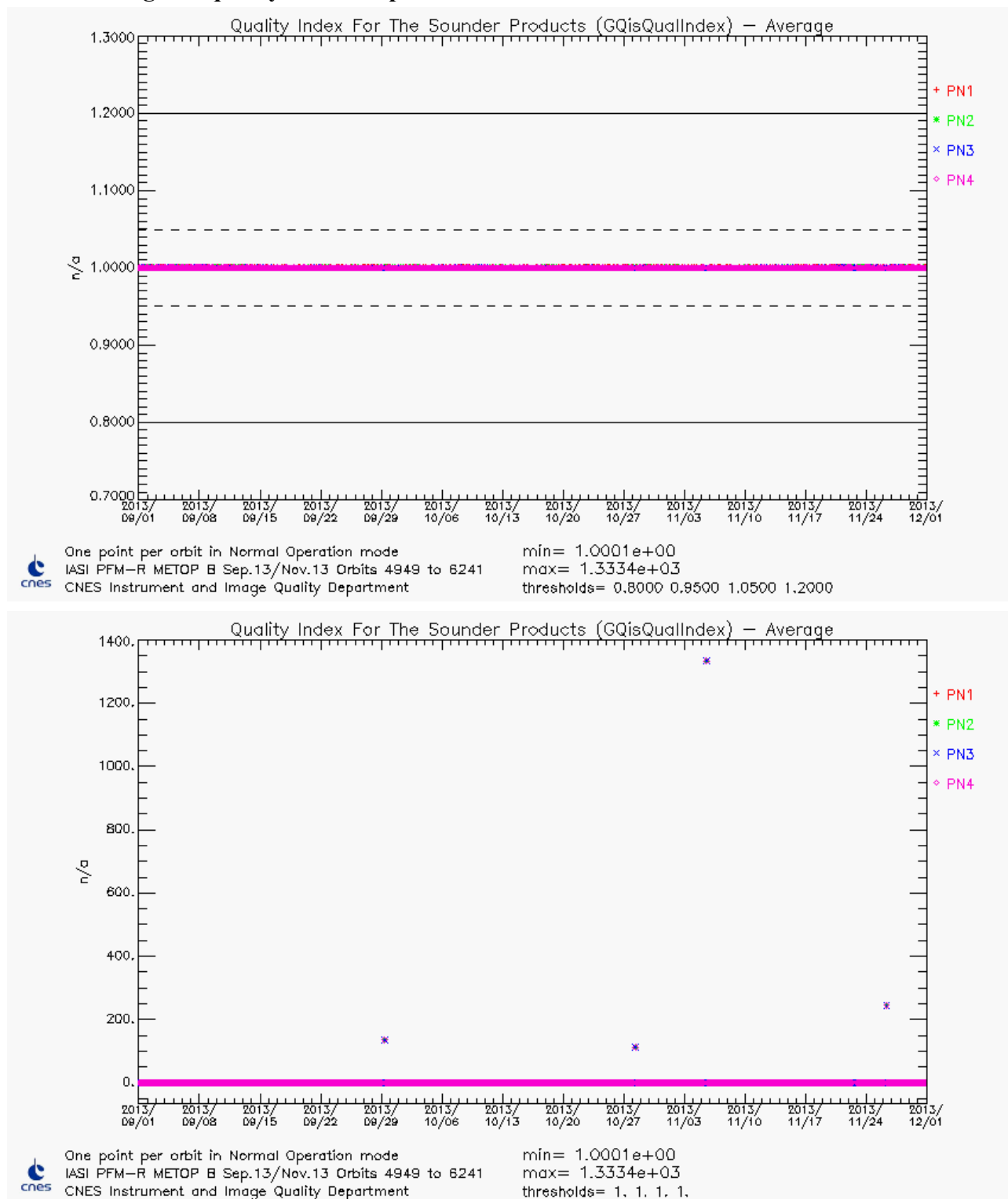




Figure 14 : GQisQualIndex average (L1 data quality index for IASI sounder)

(see 4.3.1 for peak observed on 05/11/2013 - The first figure (on top) shows the values with a fixed Y axis scale)

The high values observed each month since september 2013 happened during the monthly external calibration and a little bit after the return in normal operation. They are due to a change in the L1PPF in the FAX algorithm, where GFaxAxeRes is higher than usual when the interferometric axis guess is used. When IASI return to normal operation, the instantaneous

		Doc n°: IA-RP-2000-4122-CNE Issue: 1.0 Date: 2017-09-27 Sheet: 30 Of: 60
--	--	---

interferometric axis is a bit far from the filtered one, the distance is higher than the threshold `IDefFaxRegressRMSCutOff` and the guess is used. It is a normal and understood behavior.

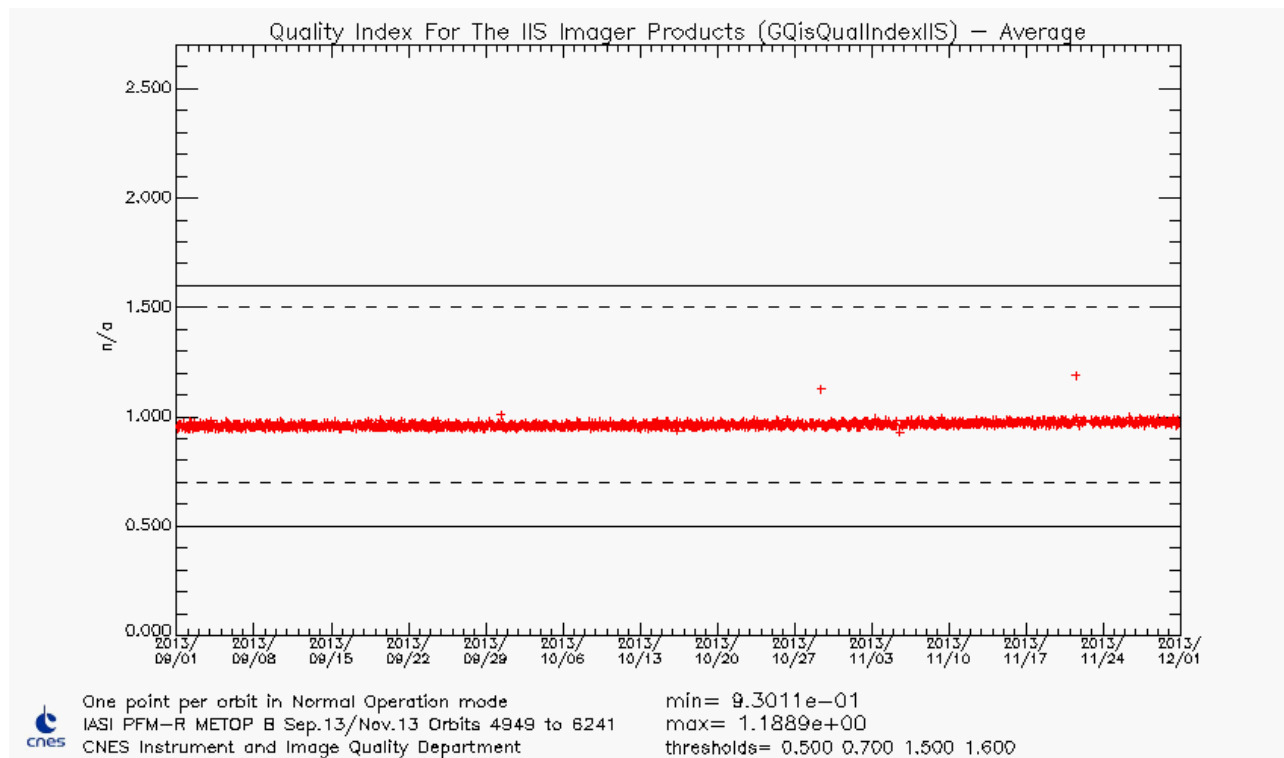


Figure 15 : GQisQualIndexIIS average (L1 data quality index for IASI Integrated Imager)

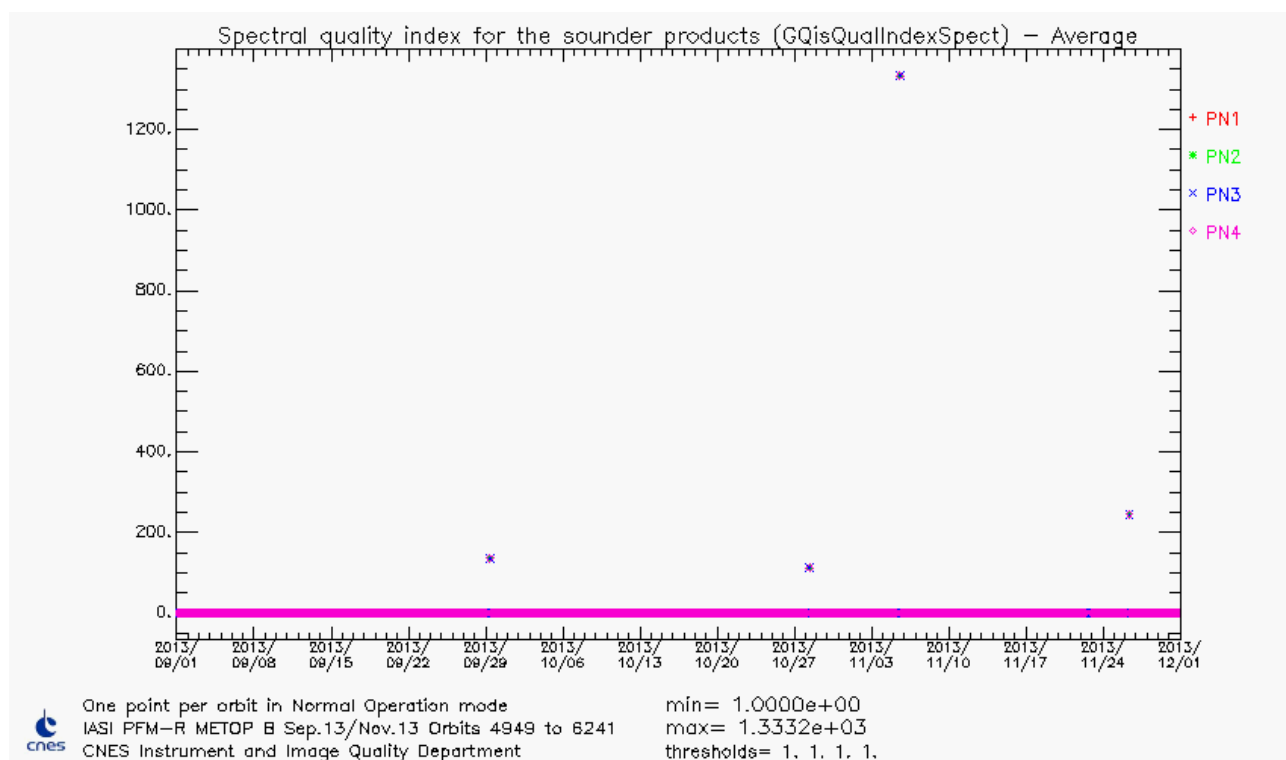
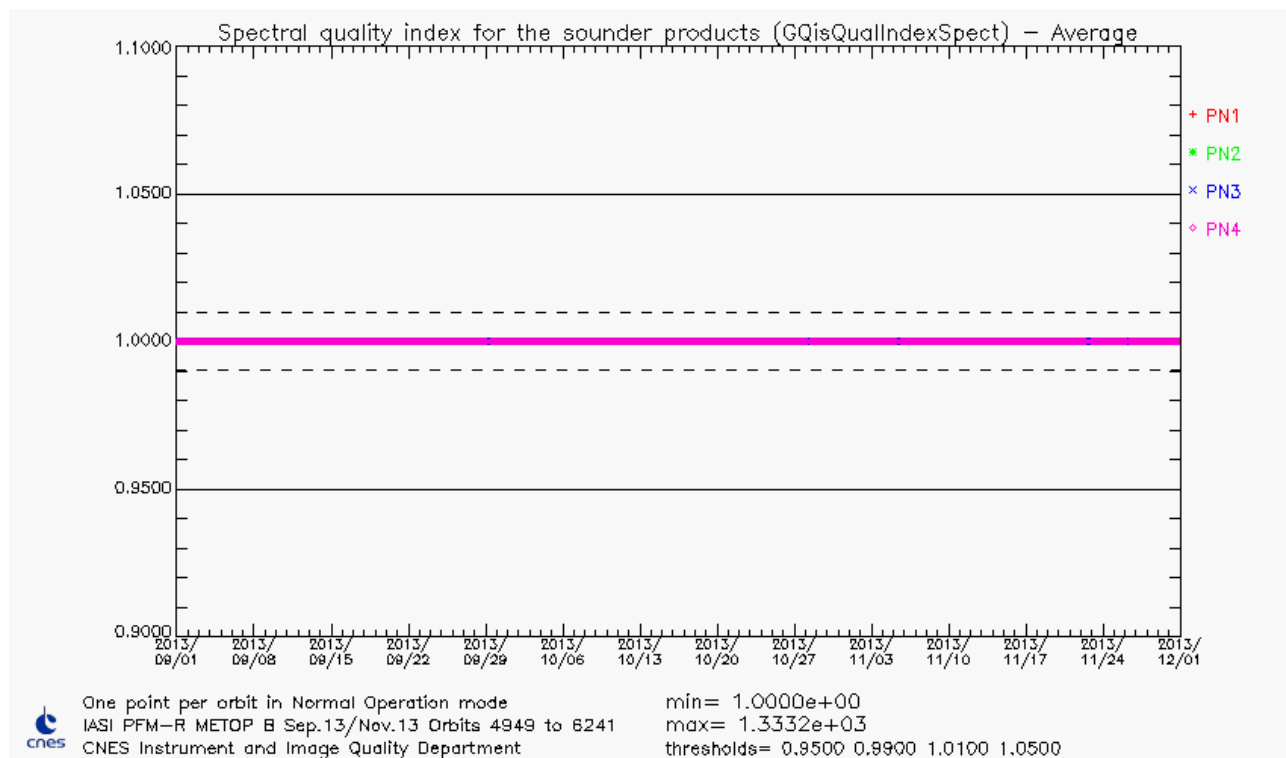


Figure 16 : GQisQualIndexSpect average (L1 data index for spectral calibration quality)

(see 4.3.1 for peak observed on 05/11/2013 - The first figure (on top) shows the values with a fixed Y axis scale)

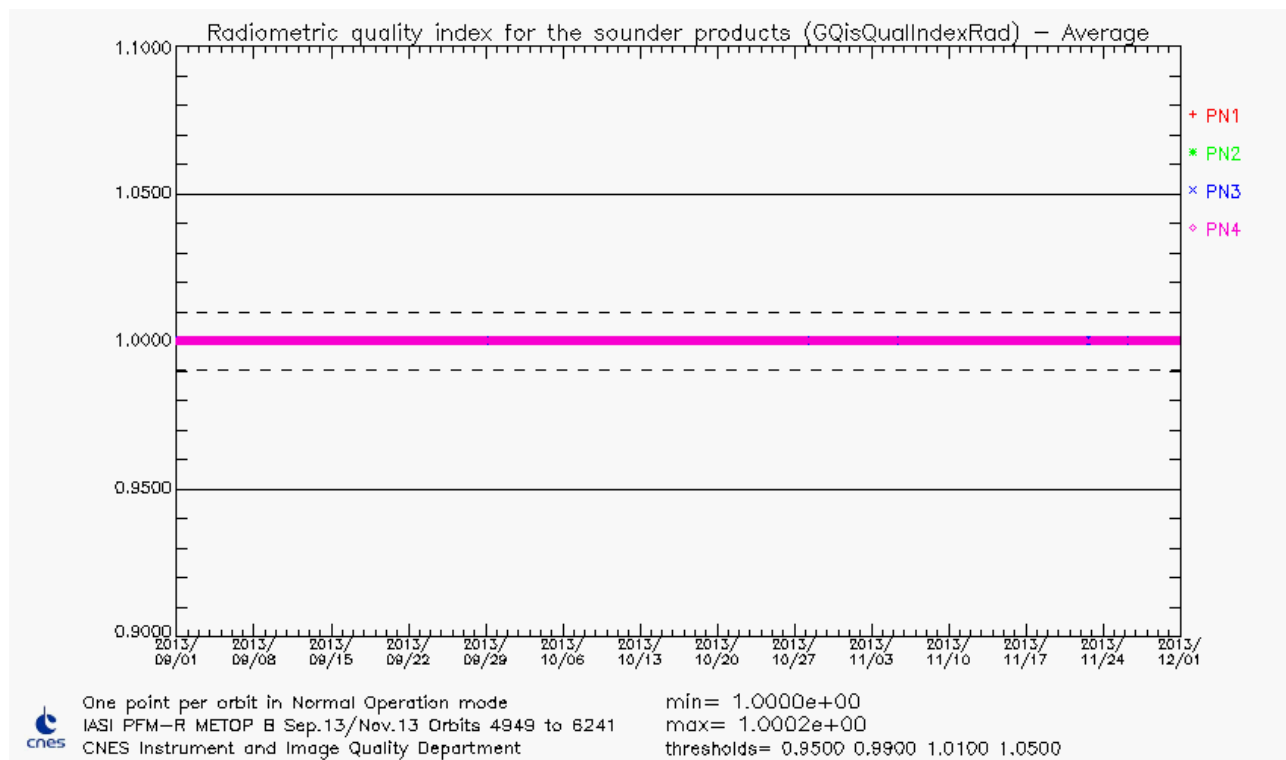




Figure 17 : GQisQualIndexRad average (L1 data index for radiometric calibration quality)

		Doc n°: IA-RP-2000-4122-CNE Issue: 1.0 Date: 2017-09-27 Sheet: 33 Of: 60
---	---	---

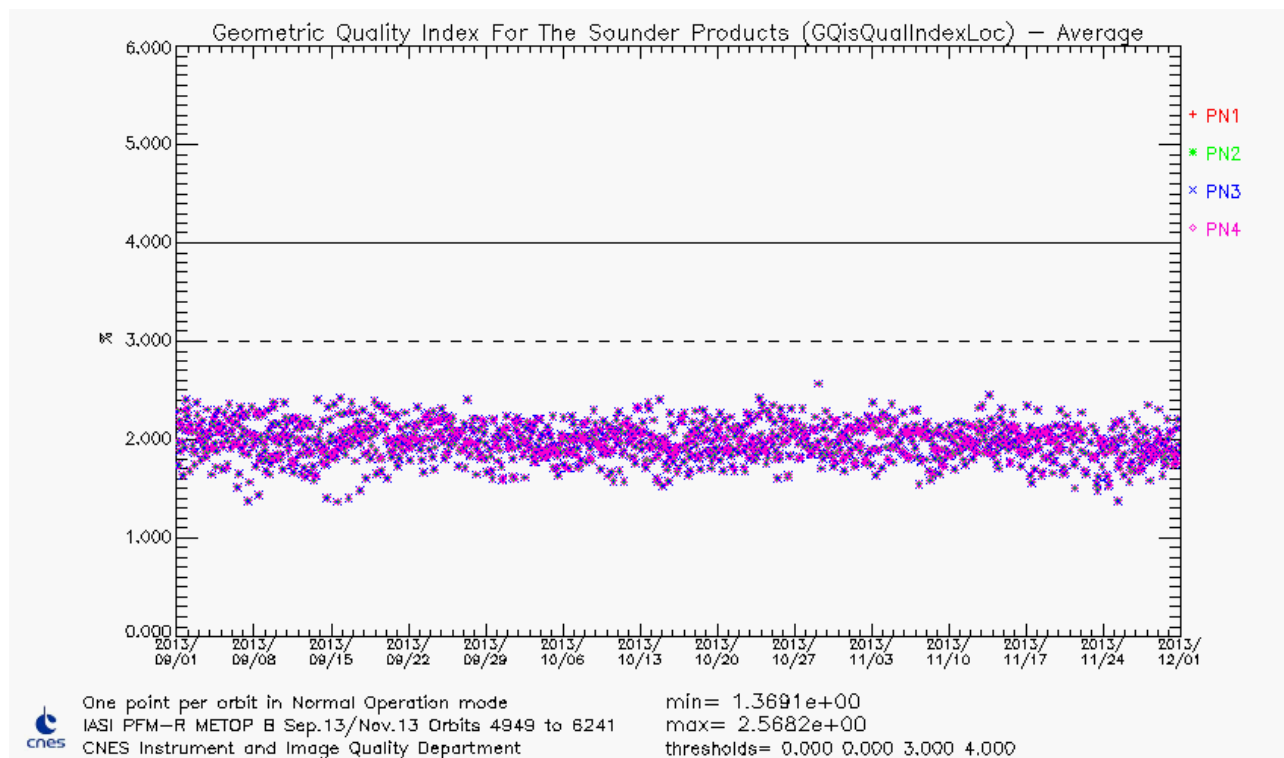


Figure 18 : *GQisQualIndexLoc* average (L1 data index for ground localisation quality)

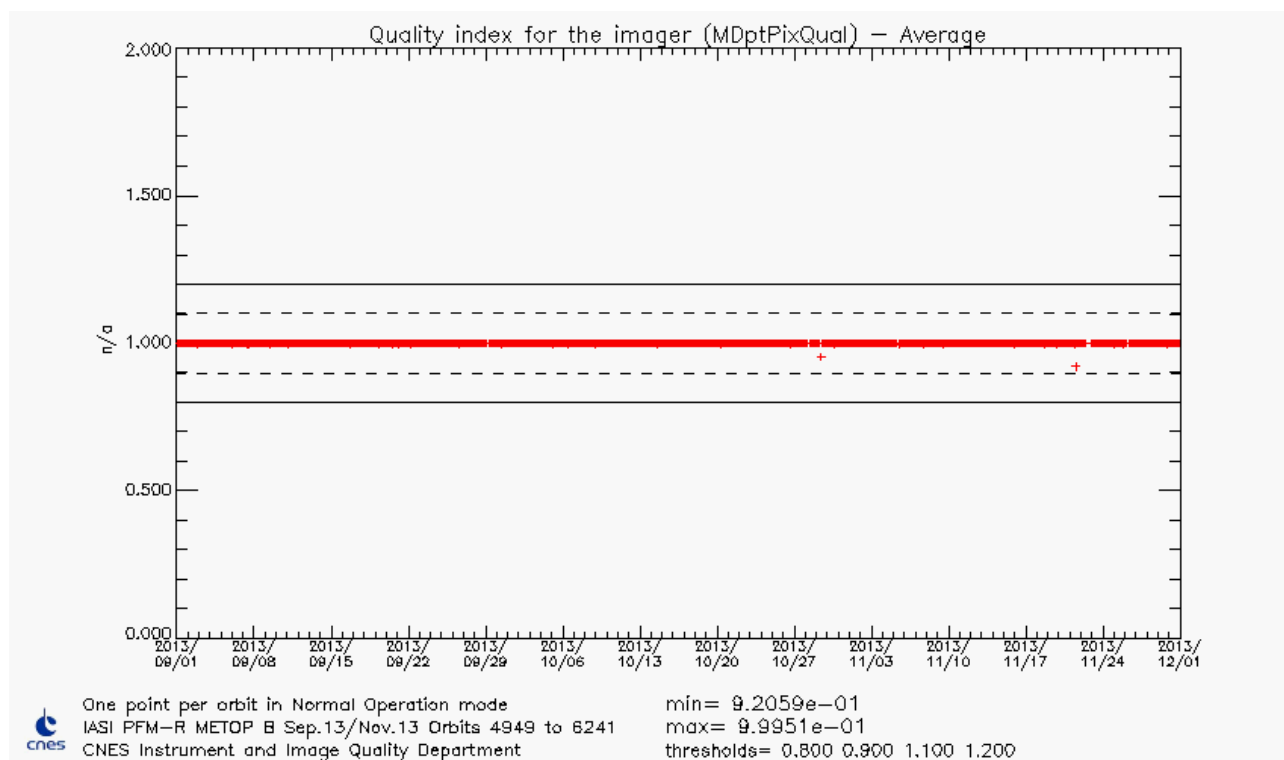


Figure 19 : *MDptPixQual* average (L1 quality index for IASI integrated imager; fraction of not dead pixels)

4.4.3 Conclusion

L1 Flag and quality indicators are stable and meet the specifications.

4.5 SOUNDER RADIOMETRIC PERFORMANCES

4.5.1 Radiometric Noise

Monitoring the radiometric noise allows to monitor the long term degradation of the instrument as well as to look for punctual anomaly of IASI or other component of METOP.

Monthly noise estimation (CE)

This monthly estimation is performed during routine External Calibration on BB views.

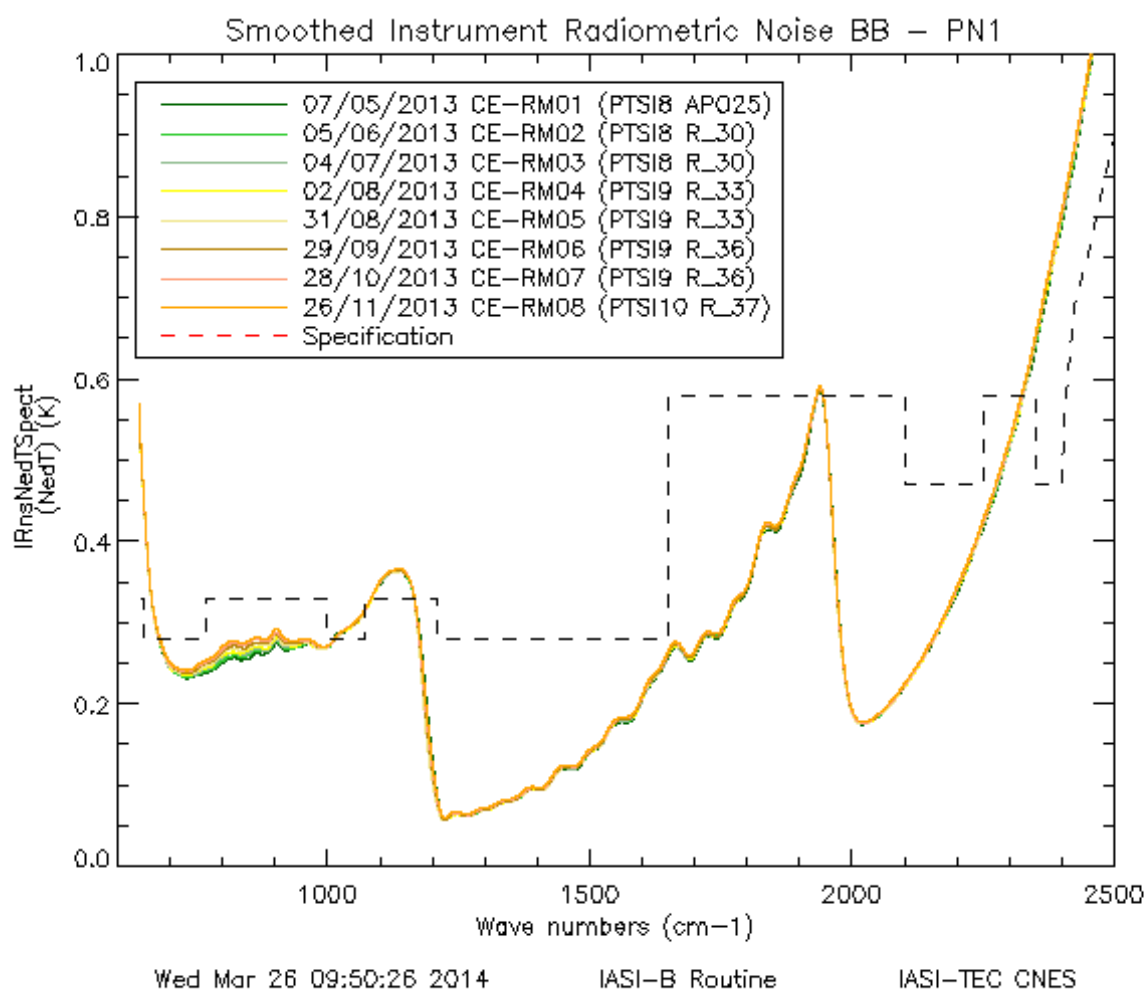




Figure 20 : Instrument noise evolution between start and end of the period

The instrument noise is very stable apart from ice effect between 700 and 1000 cm^{-1} . This point will be developed in section 4.5.4.1.

4.5.2 Radiometric Calibration

The radiometric calibration allows one to convert an instrumental measurement into a physical value. As far as IASI is concerned, the radiometric calibration is used to convert an interferogram into an absolute energy flux by taking into account instrument discrepancies. Even if the calibration has been studied on ground, it has to be continuously monitored in-flight in order to follow any potential degradation of the instrument (optics, detectors ...).

		Doc n°: IA-RP-2000-4122-CNE Issue: 1.0 Date: 2017-09-27 Sheet: 35 Of: 60
---	---	---

Approach: Radiometric fine characterization has been done during ground testing and Cal/Val. All parameters likely to cause a failure in radiometric calibration process have been identified and are continuously monitored. As long as they remain stable, there is no problem with radiometric calibration.

Evolution of scanning mirror reflectivity

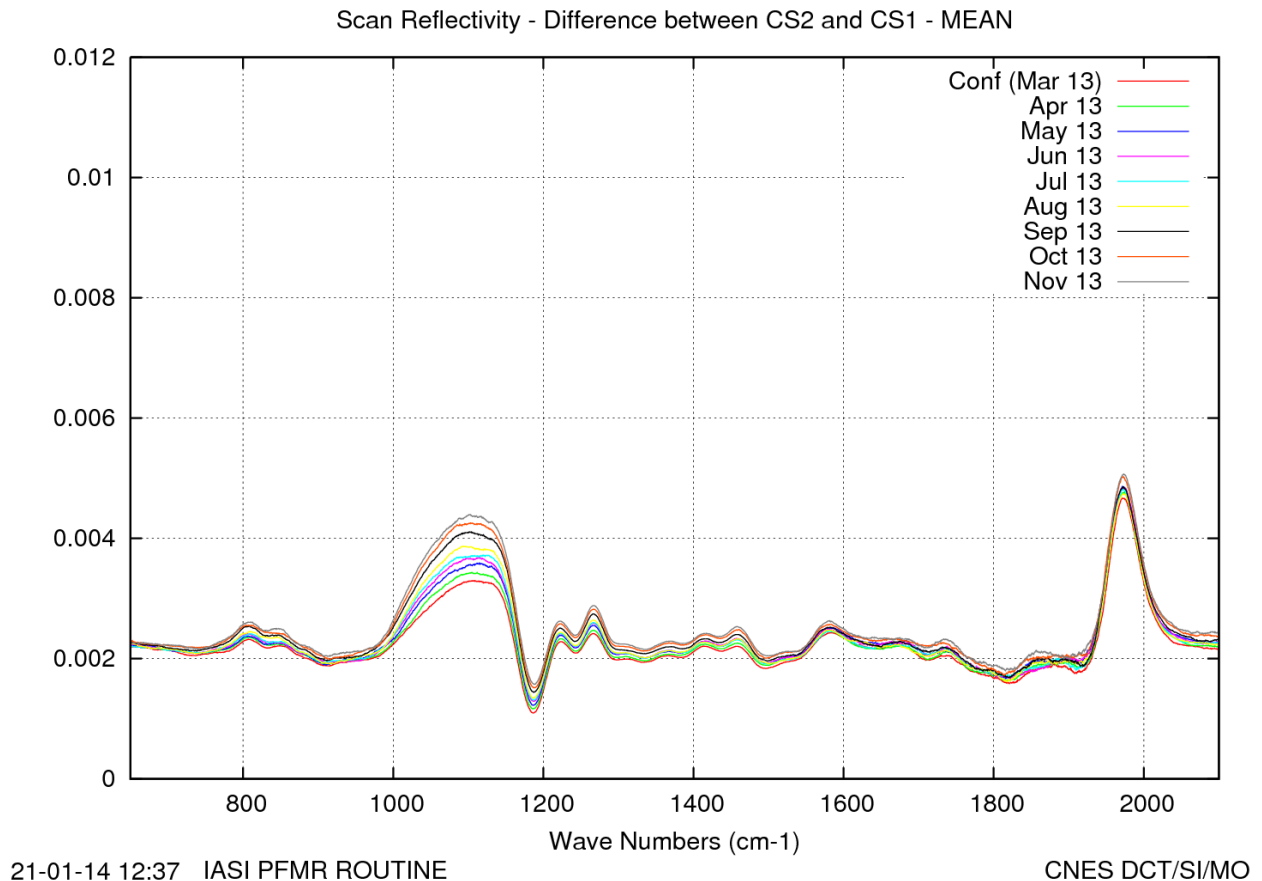
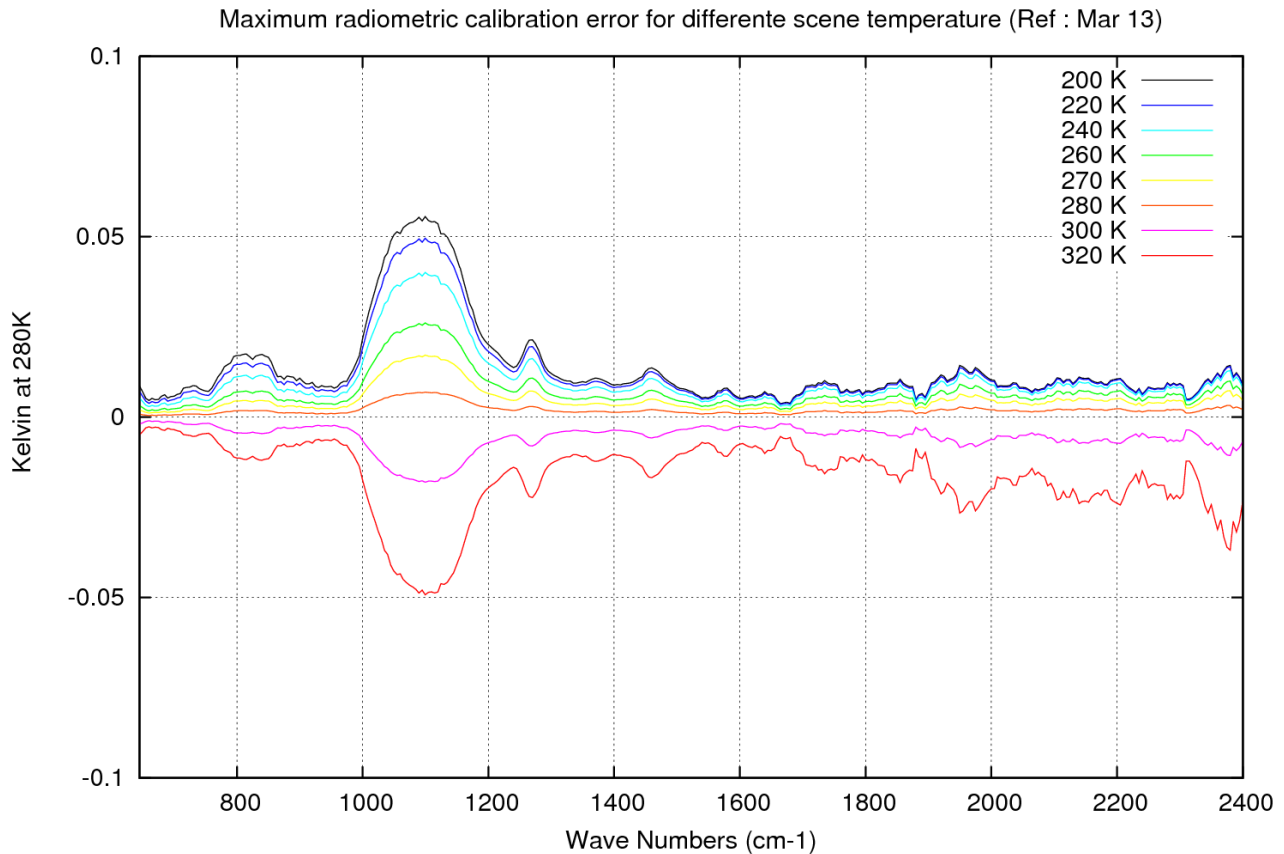


Figure 21 : Scan mirror reflectivity evolution

The reference reflexivity (in red) is the one computed on data from March 5th 2013. We see a slight evolution within [1000-1100 cm⁻¹] band. Values for wavenumbers greater than 2400 cm⁻¹ are not significant because of instrument noise.

The next figure shows the translation of scan mirror reflectivity in terms of maximum radiometric calibration error for different scene temperatures.



21-01-14 12:37 IASI PFMR ROUTINE

CNES DCT/SI/MO

*Figure 22 : Radiometric calibration error due to scan mirror reflectivity dependency
with viewing angle Maximum effect on SN1 for different scene temperature.
Done with the period May / November*

In any cases radiometric calibration maximum error is lower than the specification (0.1K). The scan mirror reflectivity law (on ground configuration), prepared with March 5th routine External Calibration data, has been updated in the operational ground segment on May 14th 2013.

Internal black body

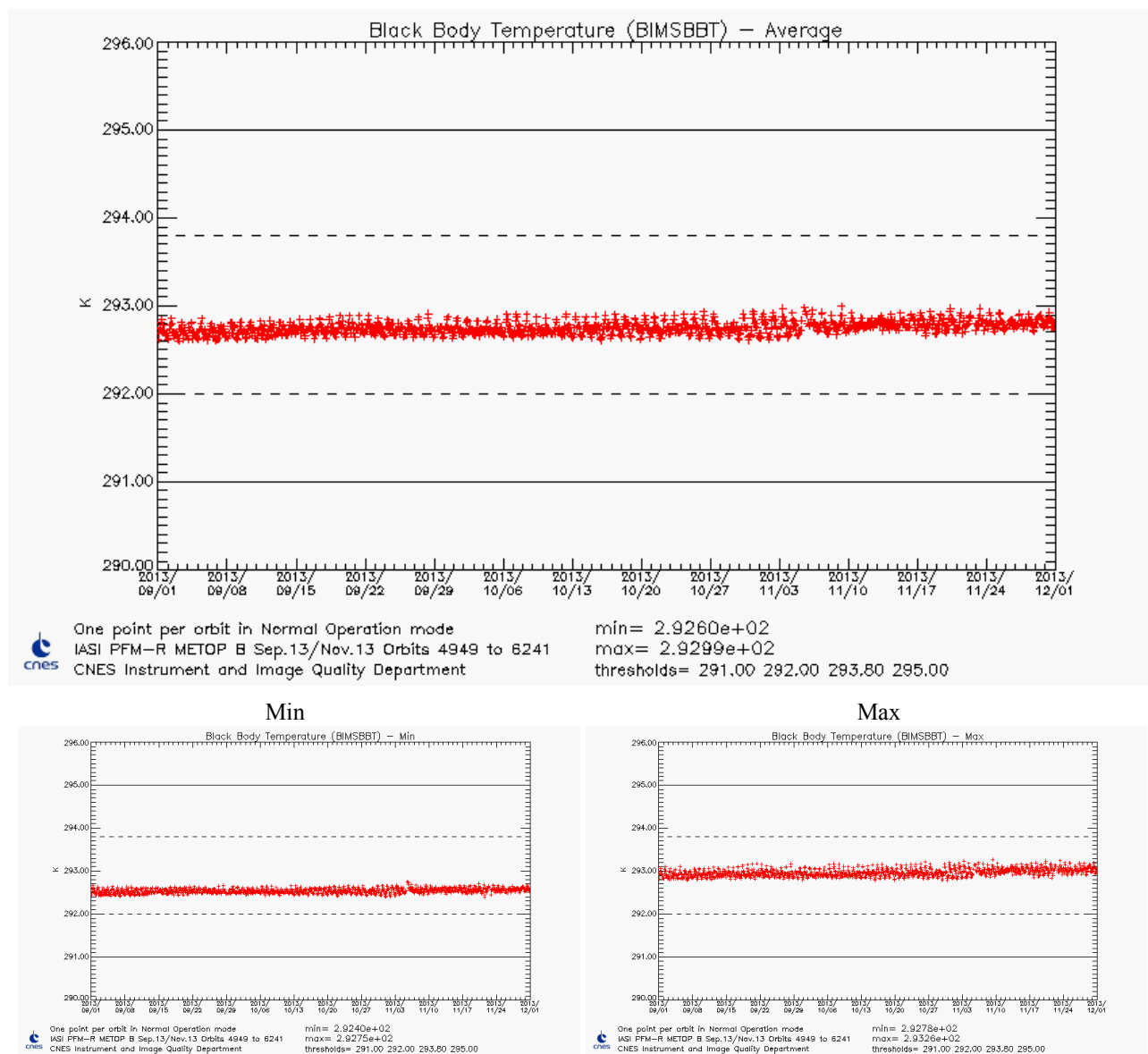




Figure 23 : Black Body Temperature

		Doc n°: IA-RP-2000-4122-CNE Issue: 1.0 Date: 2017-09-27 Sheet: 38 Of: 60
--	--	---

Non linearity of the detection chains

Non-linearity tables of the detection chains are still nominal as long as sounder focal plane temperature variation amplitude is lower than 1K.

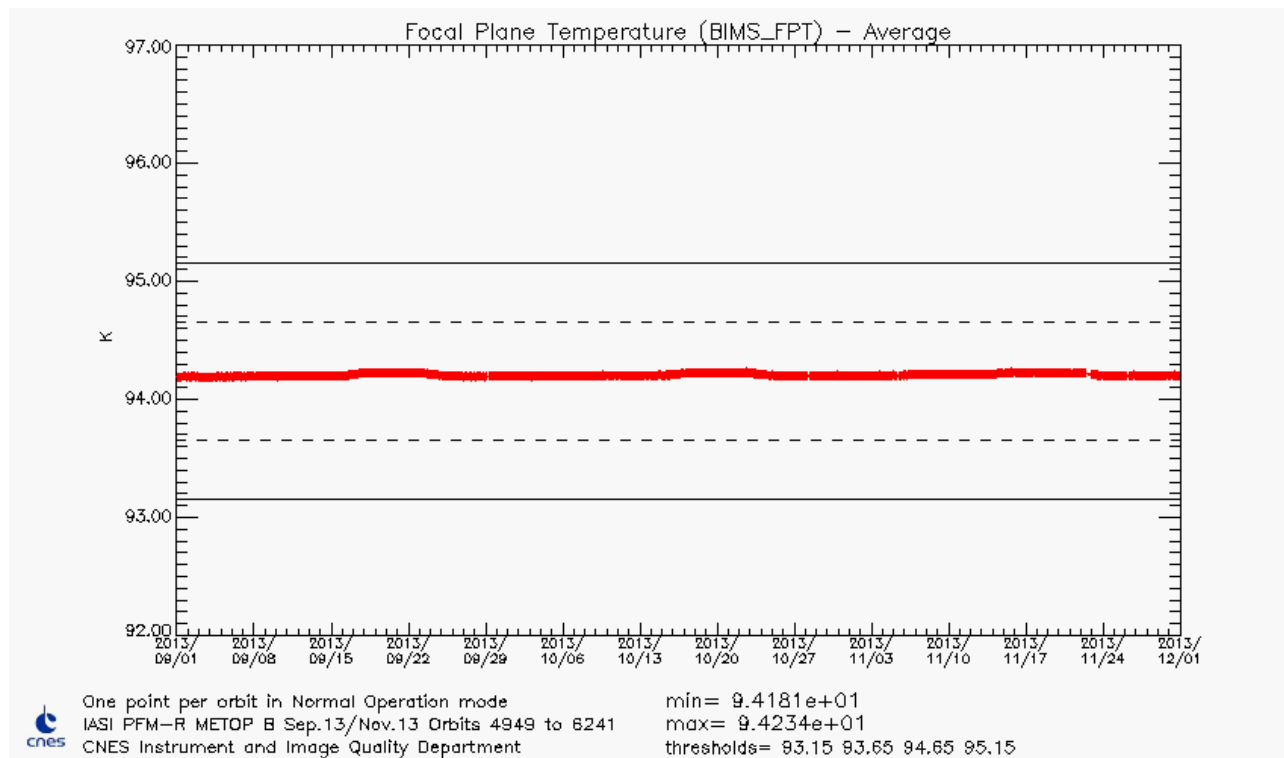




Figure 24 : Focal Plane Temperature

		Doc n°: IA-RP-2000-4122-CNE Issue: 1.0 Date: 2017-09-27 Sheet: 39 Of: 60
---	---	---

4.5.3 Delay of detection chains

Long term stability and values lower than 400 ns are required in order to properly take into account cube corner velocity fluctuations.

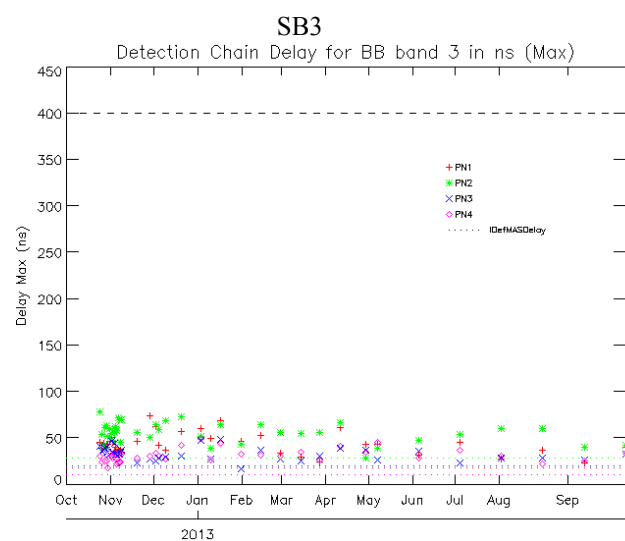
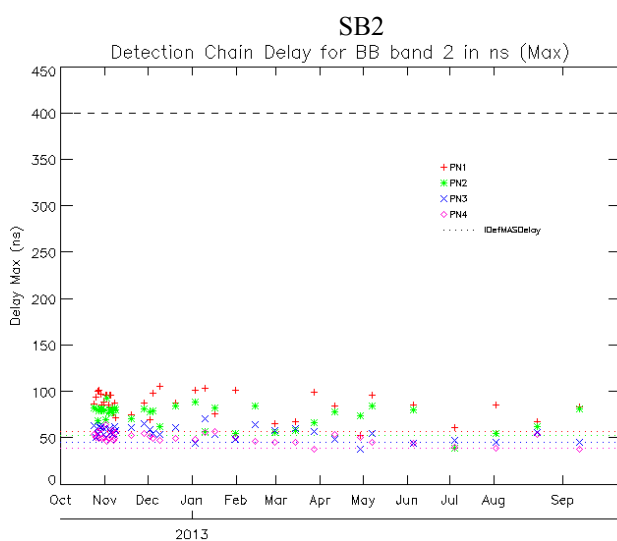
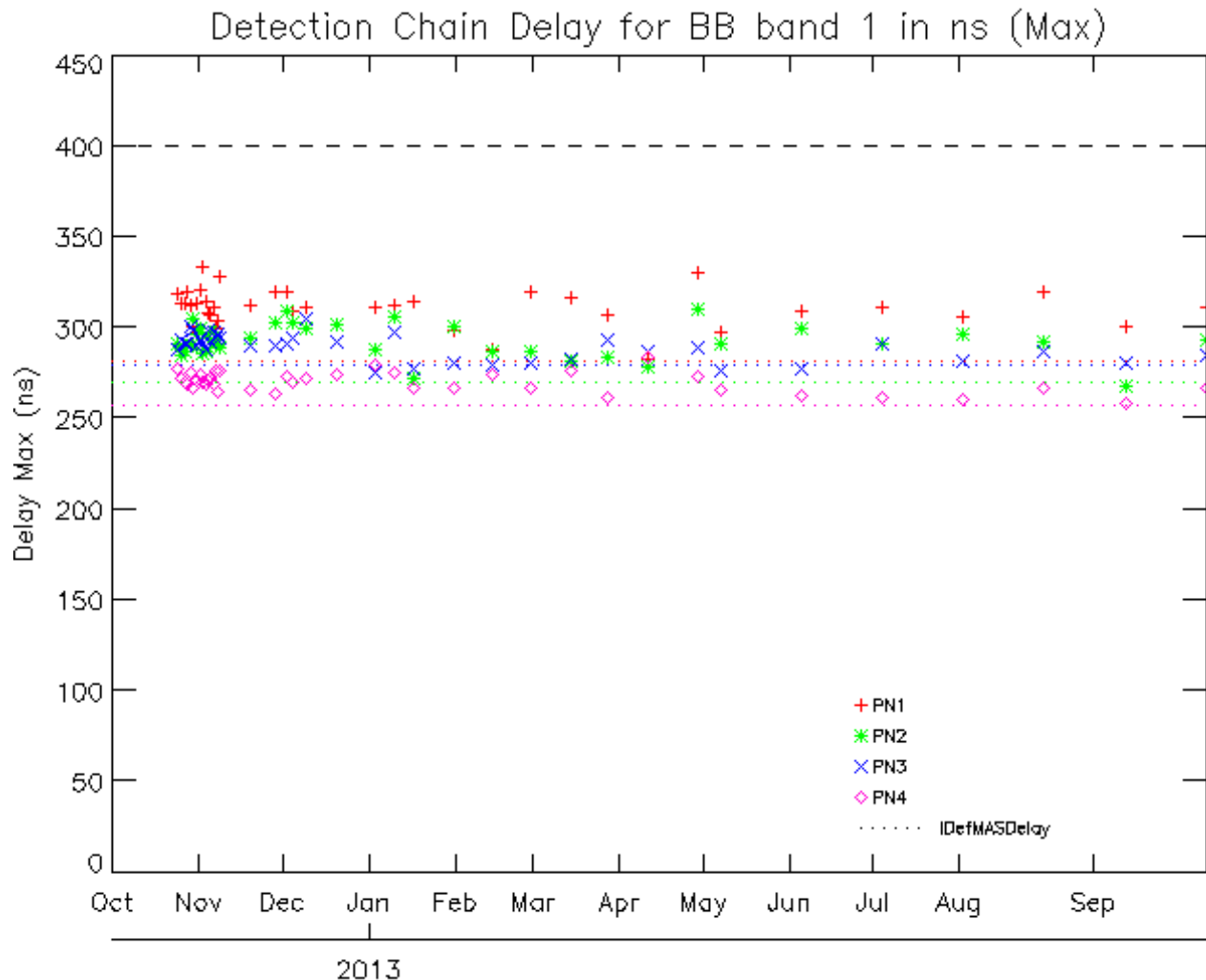




Figure 25 : Monitoring of detection chain maximum delays for all bands

		Doc n°: IA-RP-2000-4122-CNE Issue: 1.0 Date: 2017-09-27 Sheet: 40 Of: 60
---	---	---

4.5.4 Optical Transmission

4.5.4.1 Ice

The IASI interferometer and optical bench are regulated at 20°C temperature, while the cold box containing cold optics and detection subsystem is at about -180°C. Water desorption from the instrument causes ice formation on the field lens at the entrance of IASI cold box. This desorption phenomenon is particularly important at the beginning of the instrument in-orbit life. That's why one of the very first activities of IASI in-orbit commissioning was an outgasing phase consisting in heating the cold box up to 300 K during 20 days (from 22th September 2012 until 16th October 2012). This operation allows removing most of the initial contaminants coming from IASI and other MetOp instruments. A routine outgasing is then needed from time to time to remove ice contamination, but less and less frequently as the desorption process becomes slower.

The maximum acceptable degradation of transmission is about 20% loss at 850 cm⁻¹ (which corresponds to an ice deposit thickness of about 0.5 µm).

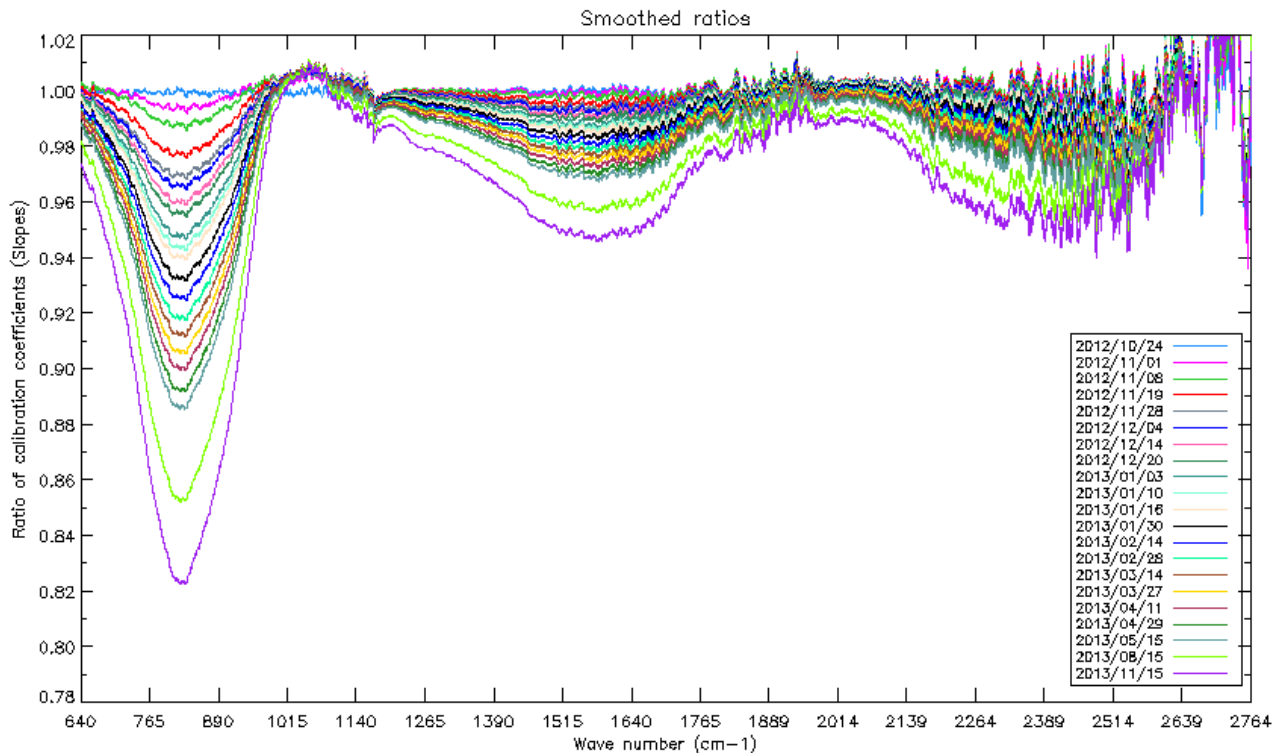




Figure 26 : Ratio of calibration coefficient slopes as a function of wave number and time after the last decontamination

		Doc n°: IA-RP-2000-4122-CNE Issue: 1.0 Date: 2017-09-27 Sheet: 41 Of: 60
--	--	---

4.5.4.2 Prediction of decontamination date

The transmission degradation rate is regularly monitored by CNES TEC through gain measurements given by calibration coefficients ratios.

The loss of instrument gain due to ice contamination is, as expected, decreasing over time. The next decontamination has been scheduled in March 2014.

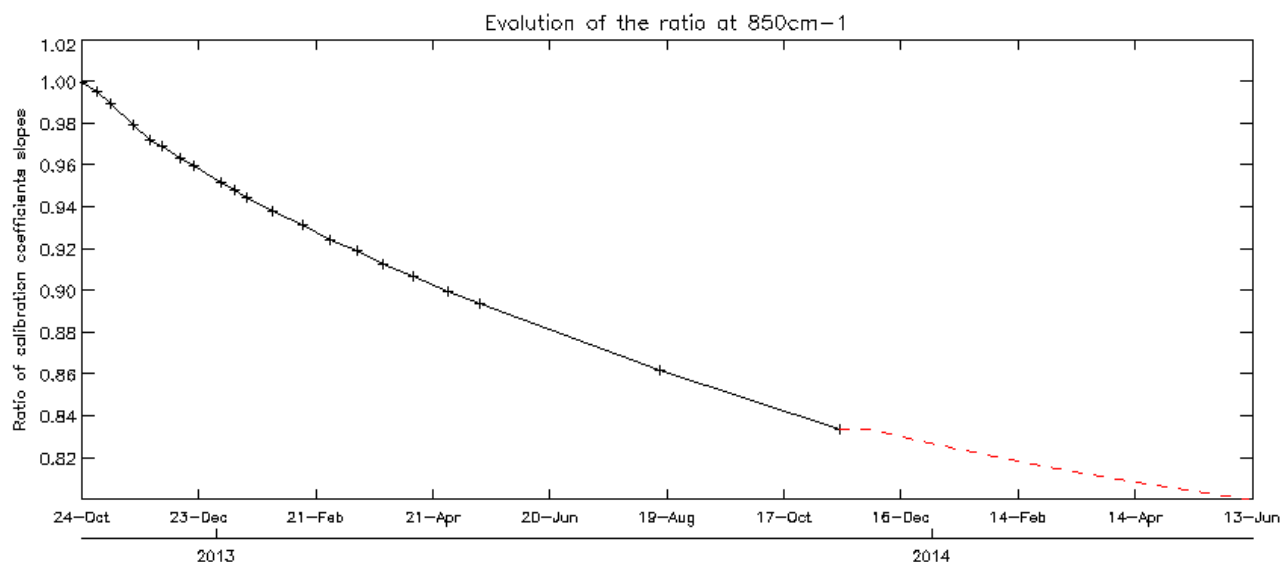


Figure 27 : Temporal evolution of calibration ratio coefficient slopes since the last decontamination. The curve was fitted with a decreasing exponential function to determine a rough date for the next decontamination (relative gain evolution of 0.8)

4.5.5 Interferometric Contrast

The interferometric contrast is defined as the interferogram fringe discrimination power. Figure 28 shows temporal evolution of instrument contrast since the beginning of IASI life in orbit for all pixels and all CCD.

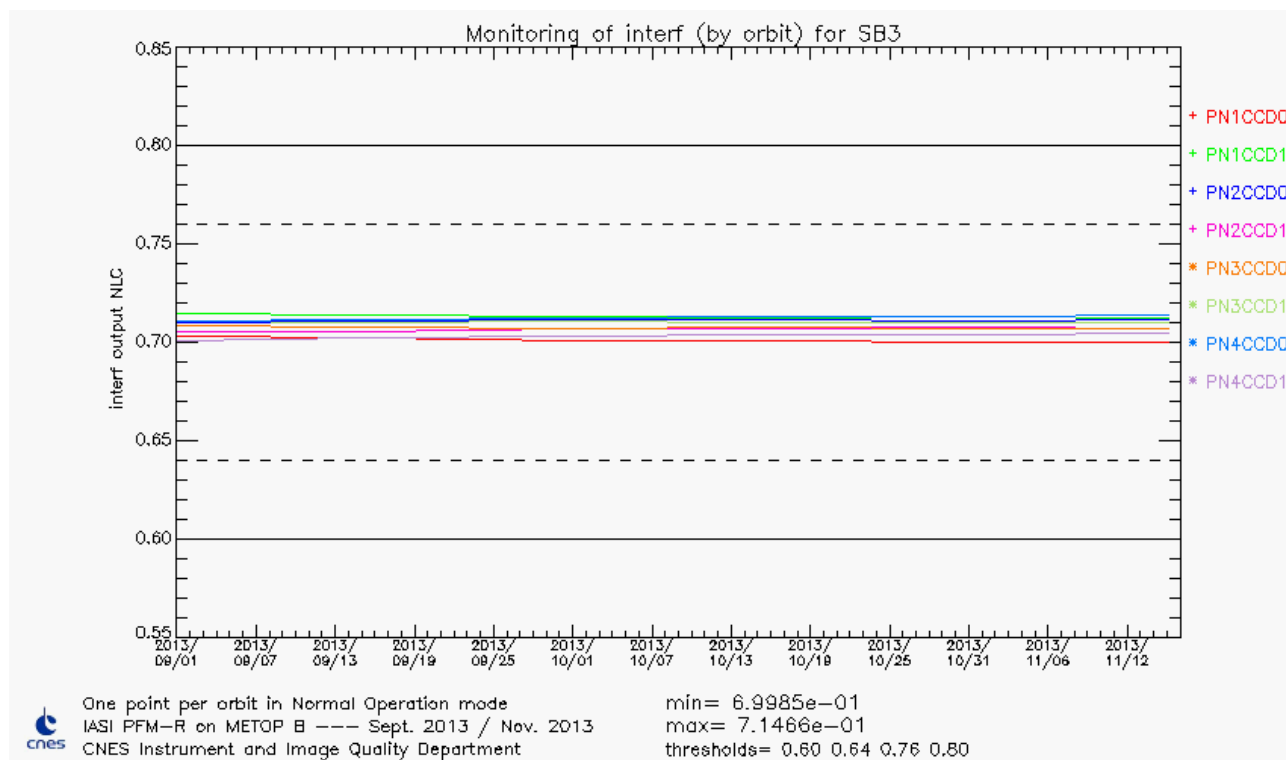




Figure 28 : Monitoring of contrast for SB3

		Doc n°: IA-RP-2000-4122-CNE Issue: 1.0 Date: 2017-09-27 Sheet: 43 Of: 60
---	---	---

4.5.6 Interferogram Baseline

The interferogram baseline is the mean value of the interferogram. Figure 29 shows temporal evolution of the baseline of the raw interferograms on calibration targets (BB and CS). The values are raw values, they are not physical, but the evolution is interesting: as the values are proportional to the energy received from a target and calibration targets are stable, the evolution can show the decrease of instrument transmission or events due to energetic particles.

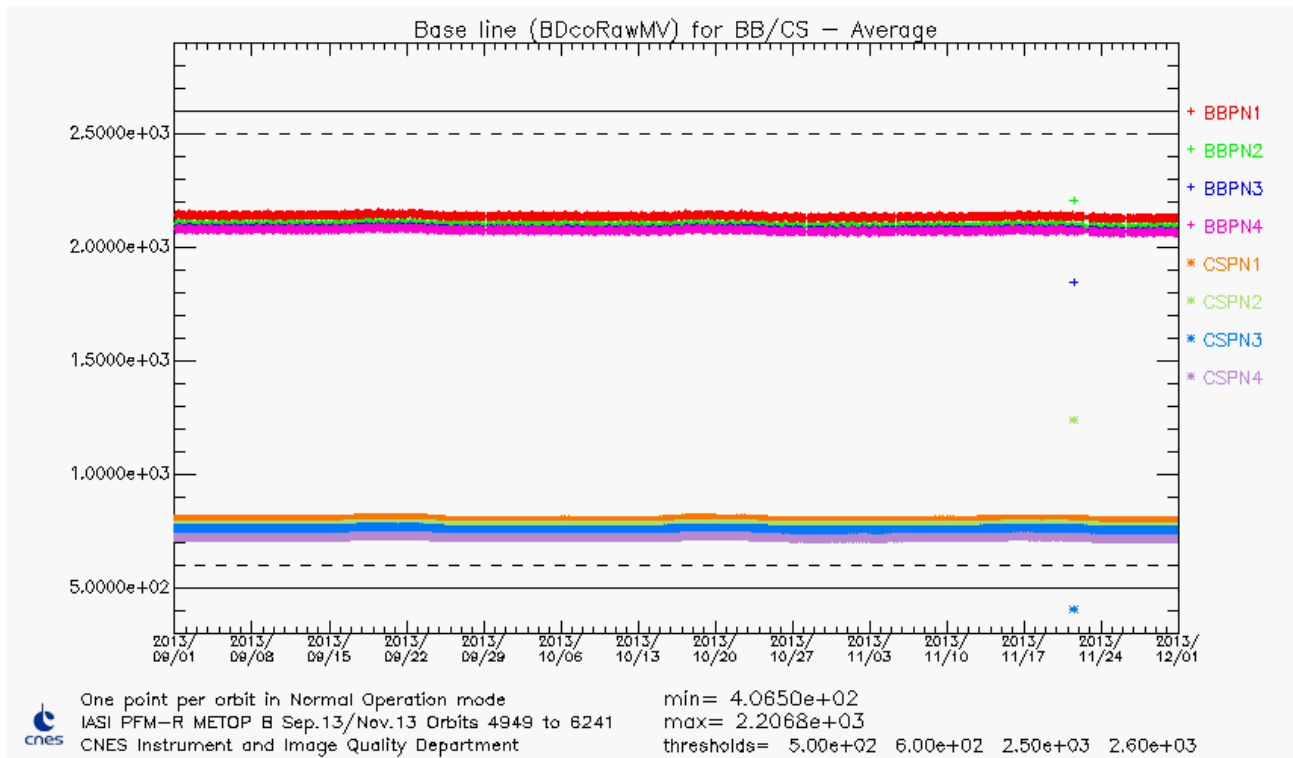




Figure 29 : Monitoring of interferogram baseline

Some high values in the temporal series are due to energetic particles that hit the detectors or the electronics and give more energy on the interferogram. This happens around 3 times per year.

		Doc n°: IA-RP-2000-4122-CNE Issue: 1.0 Date: 2017-09-27 Sheet: 44 Of: 60
---	---	---

4.5.7 Detection Chain

Detection chains are tuned in gain and offset via telecommand. The goal is to avoid saturation while conserving the maximum dynamic to limit digitalization noise.

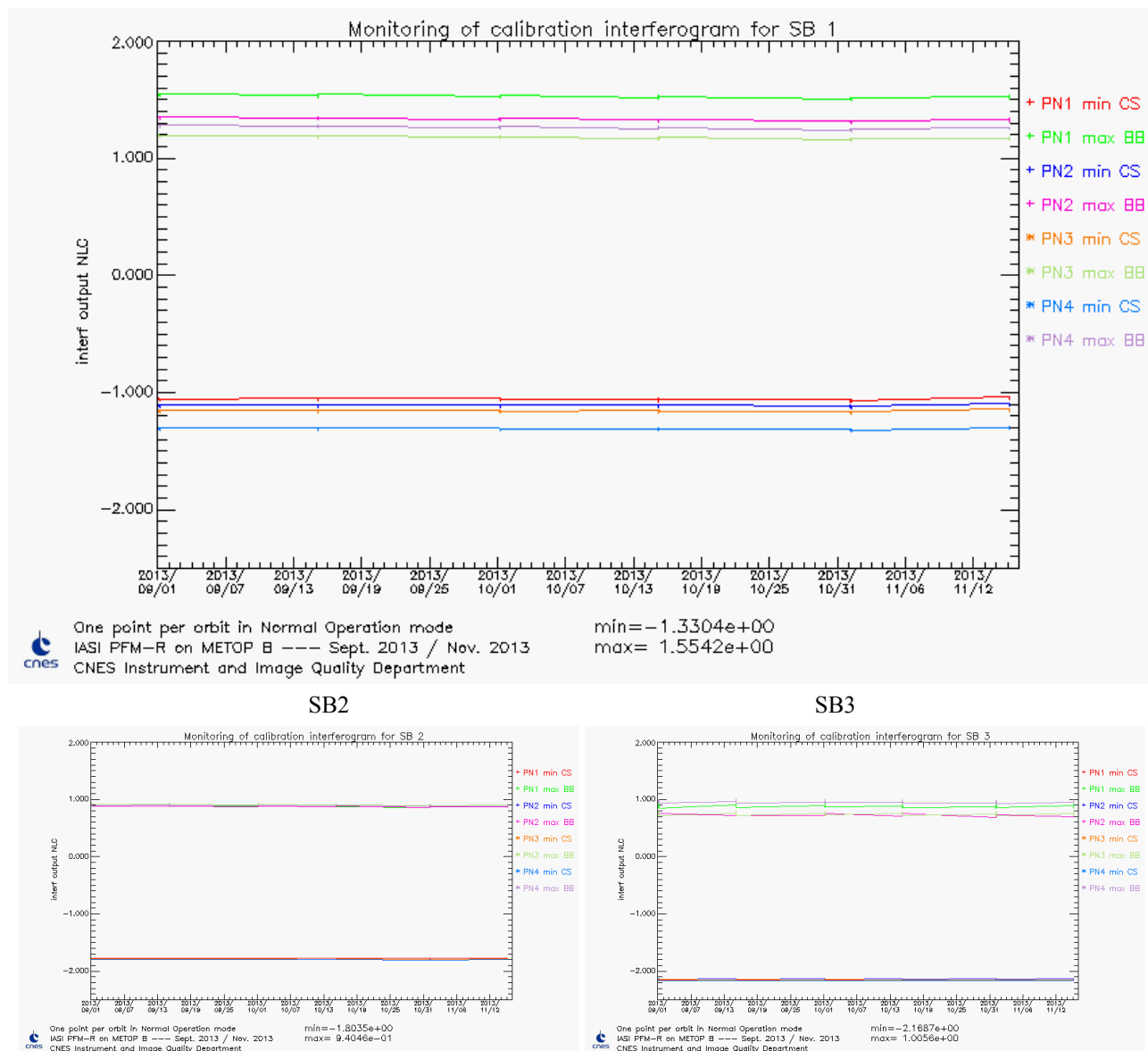




Figure 30 : Monitoring of detection chain margins

Margins are sufficient for the moment. The slight decreasing slope in SB1 (BB) for all pixels is linked to the instrument transmission evolution already mentioned in §4.5.3.1.

4.5.8 Conclusion

The radiometric performances of IASI are nominal and stable. An extrapolation of the current calibration ratio leads to a rough date for the next decontamination in March 2014. Scan mirror reflectivity was updated in May 2013. The next update is not foreseen before mid 2014.

		Doc n°: IA-RP-2000-4122-CNE Issue: 1.0 Date: 2017-09-27 Sheet: 45 Of: 60
---	---	---

4.6 *SOUNDER SPECTRAL PERFORMANCES*

This part is specific to hyperspectral sounders. The goal of the spectral calibration is to provide the best estimates of spectral position of the 8461 IASI channels.

The large sensitivity of infrared spectrum to spectral calibration errors has lead to stringent specifications:

- A prior knowledge of spectral position better than of $2 \cdot 10^{-4}$ (design)
- A posterior maximum spectral calibration relative error of $2 \cdot 10^{-6}$ (after calibration by OPS)

In order to reach the specification of $2 \cdot 10^{-6}$, we need an accurate Instrument Spectral Response Function (ISRF) model. This model have been done and validated in the early time of IASI development.

For sake of operational time constrain, complete ISRF calculation is not done in real-time by OPS software but pre-calculated and stored in a database called “spectral database”. OPS processing determine on-line the most relevant instrument function to be used by OPS with respect to current values of a set of parameters (interferometric axis, cube corner offset...).

The approach to monitor IASI spectral performances is very similar to the one used for radiometric calibration. Spectral calibration fine characterization has been done during ground testing and Cal/Val. All parameters likely to cause a failure in spectral calibration process have been identified and are continuously monitored. As long as they remain stable, there is no problem with IASI spectral calibration.

In addition, a spectral calibration assessment is done over homogeneous scenes when IASI is in external calibration, nadir view.

4.6.1 Monitoring of the ISRF inputs

4.6.1.1 Position of the interferometric axis

The interferometric axis is the cube corner displacement direction. Its value has changed several times during CalVal due to the various configurations used. Since the end of CalVal, its value is now stable around ($Y = 1060 \mu\text{rad}$; $Z = 1210 \mu\text{rad}$). The central position used in the “spectral database” generation, are $1000 \mu\text{rad}$ and $1200 \mu\text{rad}$, respectively for Y and Z axis.

Since the drift of the interferometer axis is lower than $300 \mu\text{rad}$, there is no need to update the “spectral database”.

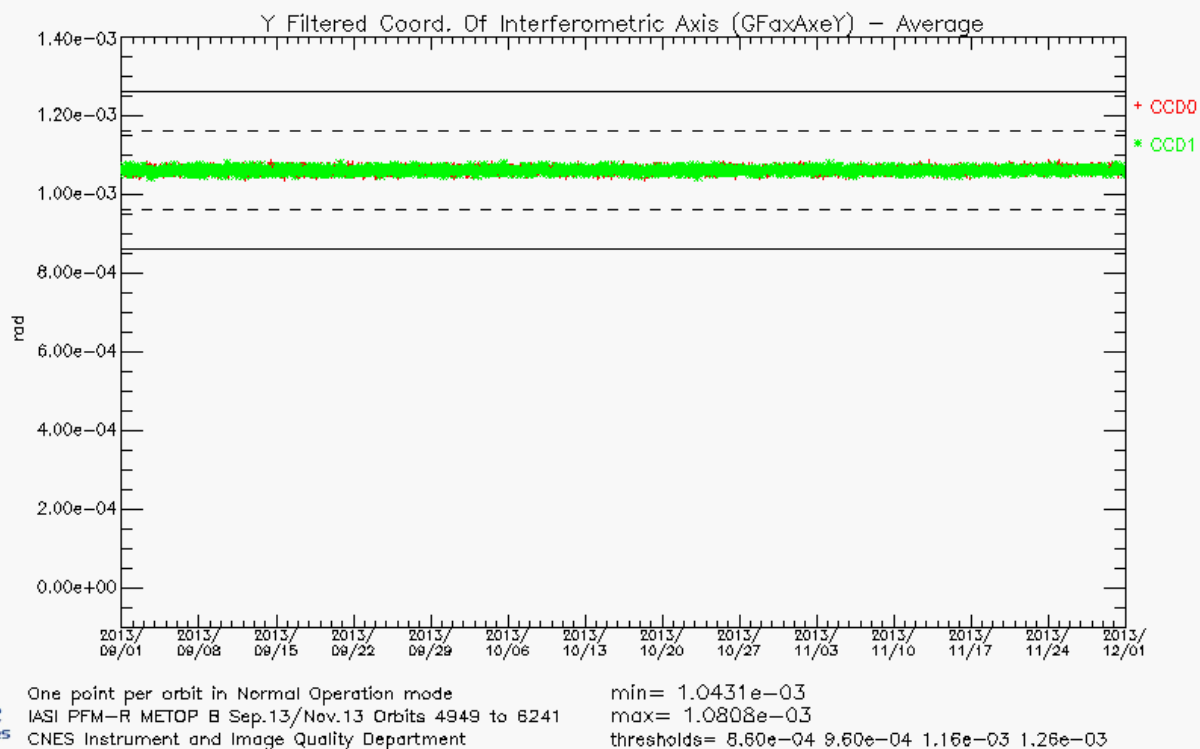
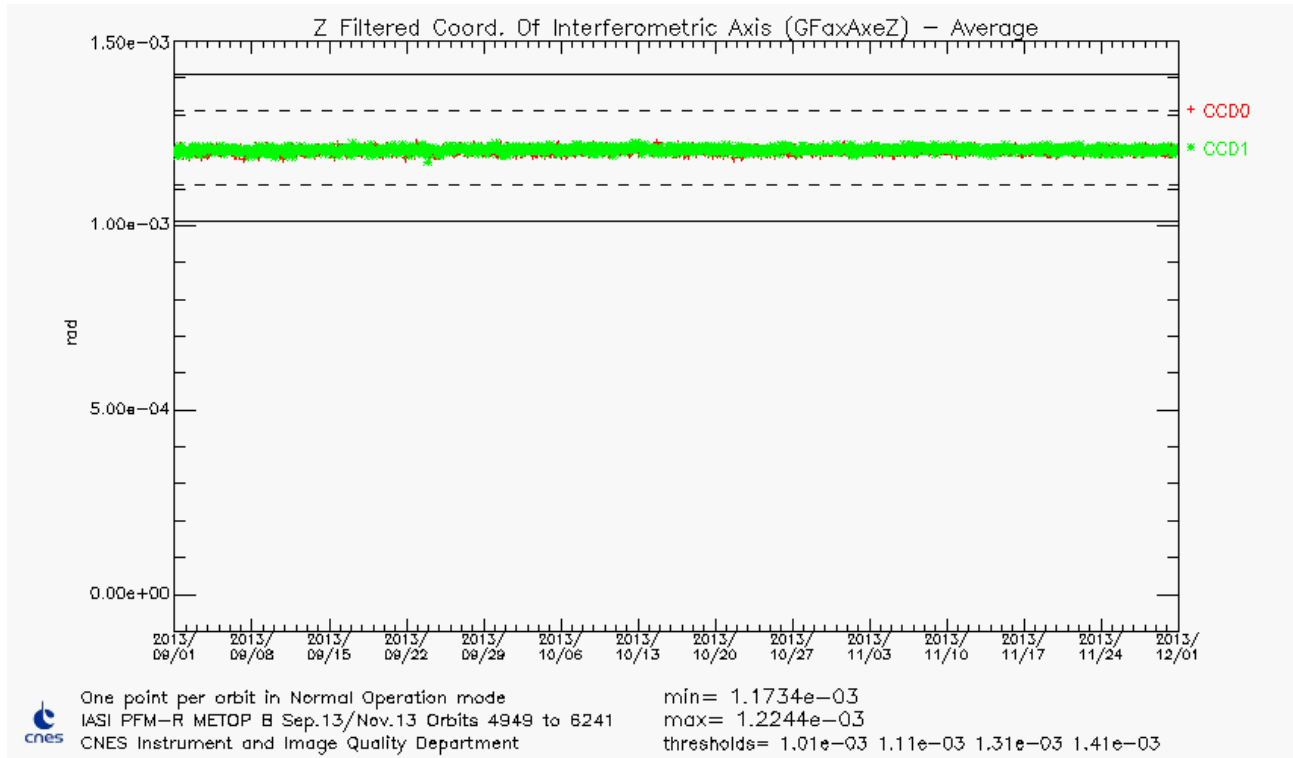
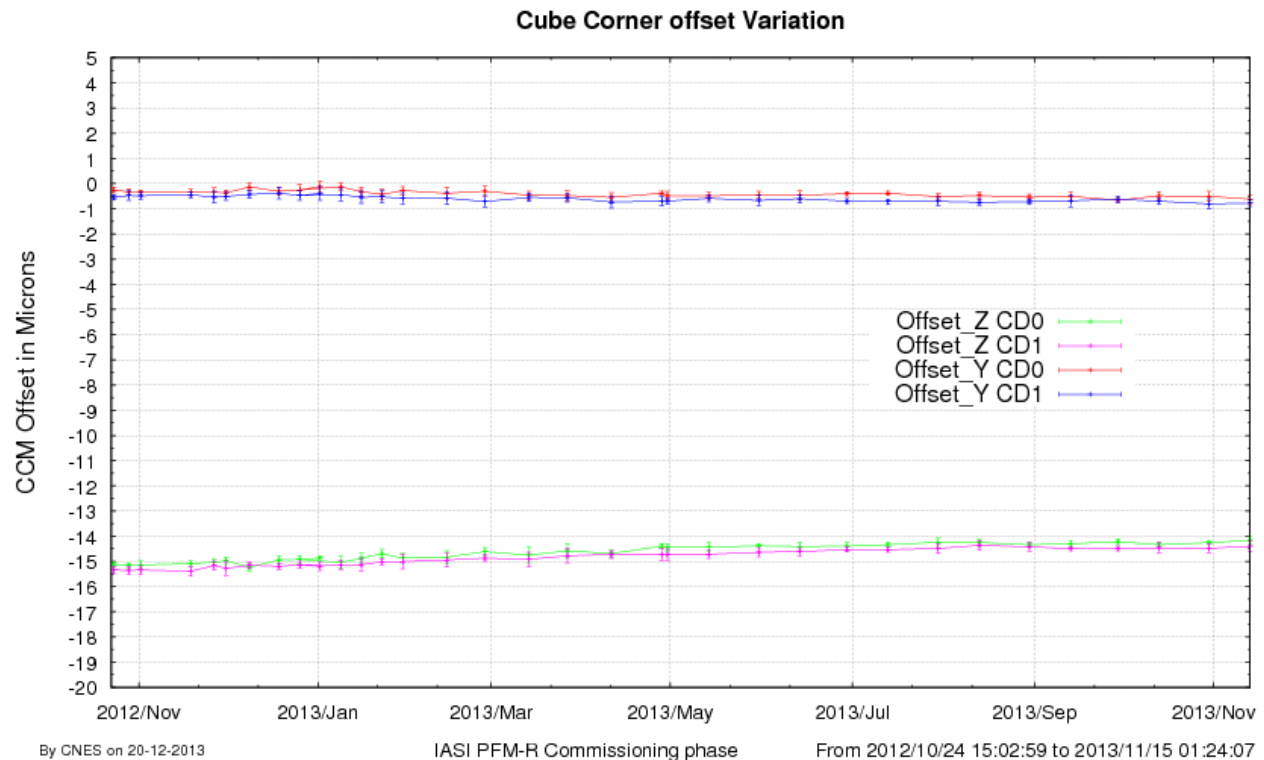




Figure 31 : GFaxAxeY average (Y filtered coordinates of sounder interferometric axis)



4.6.1.2 Cube Corner constant offset



Reference cube corner offsets, used in the spectral database of the period (ODB 12), are $-0.48 \mu\text{m}$, $-0.61 \mu\text{m}$, $-14.54 \mu\text{m}$ and $-14.64 \mu\text{m}$, respectively for Y CD0, Y CD1, Z CD0 and Z CD1.

		Doc n°: IA-RP-2000-4122-CNE Issue: 1.0 Date: 2017-09-27 Sheet: 48 Of: 60
--	--	---

Since the drift of cube corner offset is lower than 4 μm , there is no need to update the spectral database.

4.6.1.3 Cube corner velocity

Refer to REVEX, paragraph 5.5.

4.6.1.4 Interferometer optical bench temperature

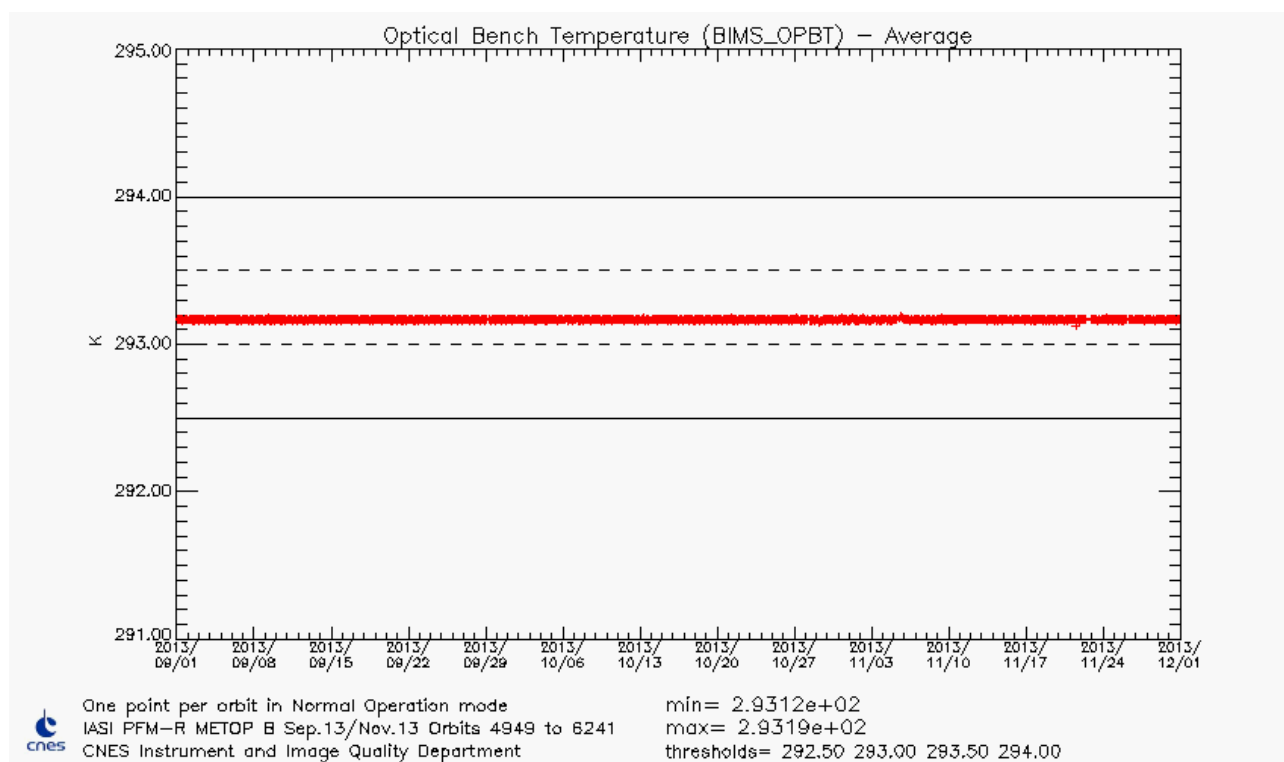


Figure 34 : Optical bench Temperature

4.6.2 Spectral calibration assessment

This assessment is performed during routine External Calibration on Earth views at nadir (SP 15).

4.6.2.1 Absolute spectral calibration assessment

IASI L1C spectra are compared with simulated spectra over homogeneous scenes, warm and clear.

The spectra are simulated with 4AOP radiative transfer model with collocated input profiles: temperature and water vapor profiles are extracted from meteorological analysis from ECMWF, the others gazes like CO₂, O₃, CO, N₂O and CH₄ profiles are extracted from a climatological data base.

The IASI spectra are selected using the pseudo channel Variance of the IIS radiance. The variance must be lower than 0.65 Kelvin, that is very close to the IIS noise level. This criterion insures a quasi-perfect homogeneity of the scenes (but not necessarily clear). The minimum of the pseudo channel IIS brightness temperature is 286K, which insures to have a hot scene, rejecting the areas where there is a lack of dynamic in the atmospheric spectral lines and rejecting the majority of cloudy scenes (which are not simulated). Then only contiguous selected scenes are kept (20 lines maximum, 1000 km).

The 4AOP spectra are simulated using the coordinates of the center of each sequence.

The comparison is done by using the correlation method in spectral windows (using the derivative of the spectrum). The position of the maximum of the correlation coefficient gives us the spectral shift. The result is expressed in terms of relative spectral shift error between L1C simulated and measured spectra for each pixel.

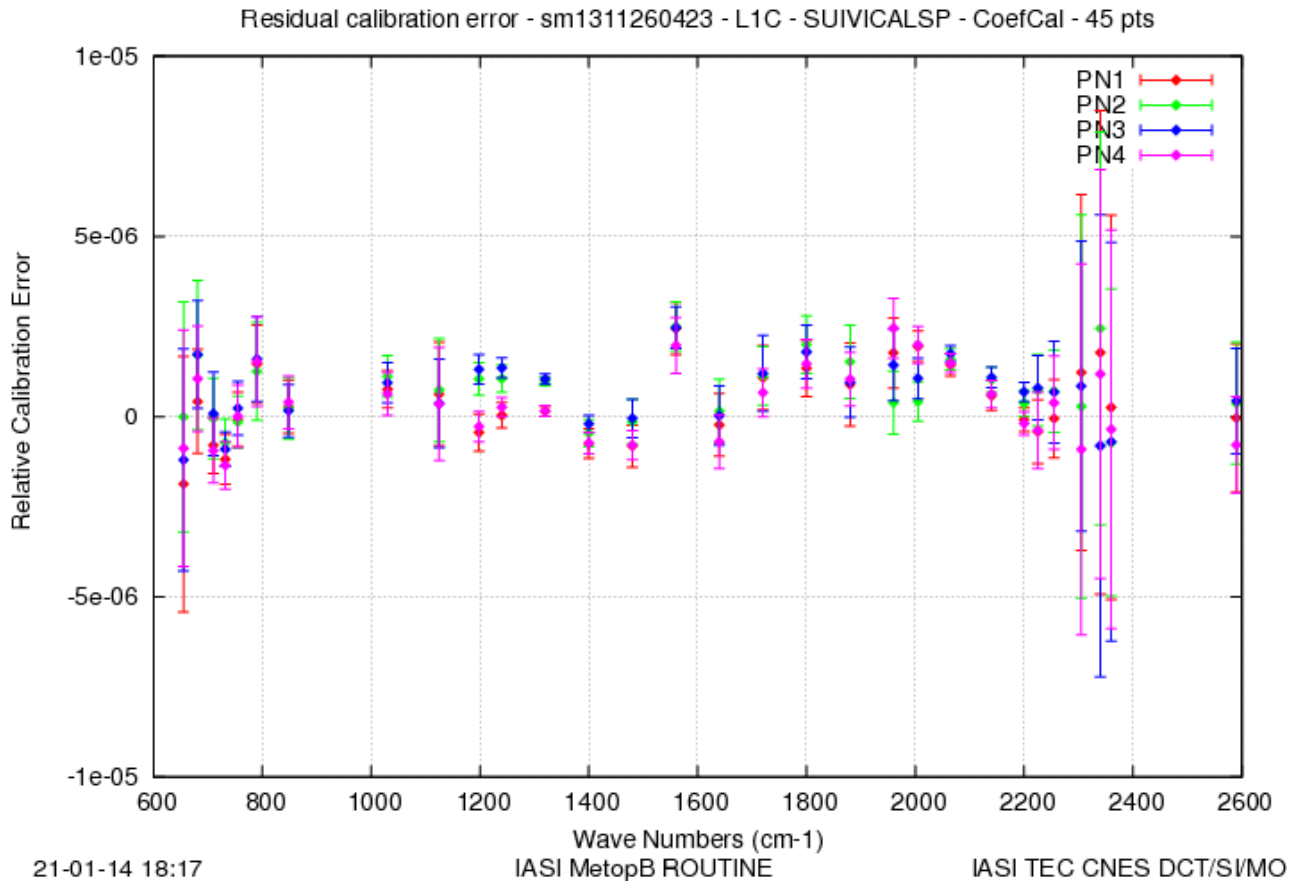


Figure 35 : Spectral shift error between L1C IASI and simulated L1C with A4/OP + ECMWF

The absolute spectral calibration assessment by comparison with a model is fully satisfactory on spectral bands that permits this exercise, the specification of 2.10^{-6} is reached.

We can note that the spectral shift in the inter-band is not good because of a sharp gradient of the spectral filters (transmission function) at the edge of spectral bands. So, the energy in a line is not the same in every channel included in the line, the barycenter of the line changes, that induces a spectral shift. For B1/B2, the inter-band limit is around 1169 cm^{-1} , and for B2/B3 it is around 1953 cm^{-1} .

The model has its limits : it is not true everywhere in the spectrum, because the geophysical conditions are not well known. For example, in B2 a bad knowledge of the water vapor content leads to a bad simulation and thus to a spectral shift in B2 only due to the variability of the water vapor. There are still improvements to make on spectroscopy and the radiative transfer models.

4.6.2.2 Interpixel spectral calibration assessment

Over the same homogeneous scenes used for absolute spectral calibration assessment, IASI L1C spectra of each pixel are compared with the average spectra of all pixels. The result is expressed in terms of interpixel relative spectral shift error.

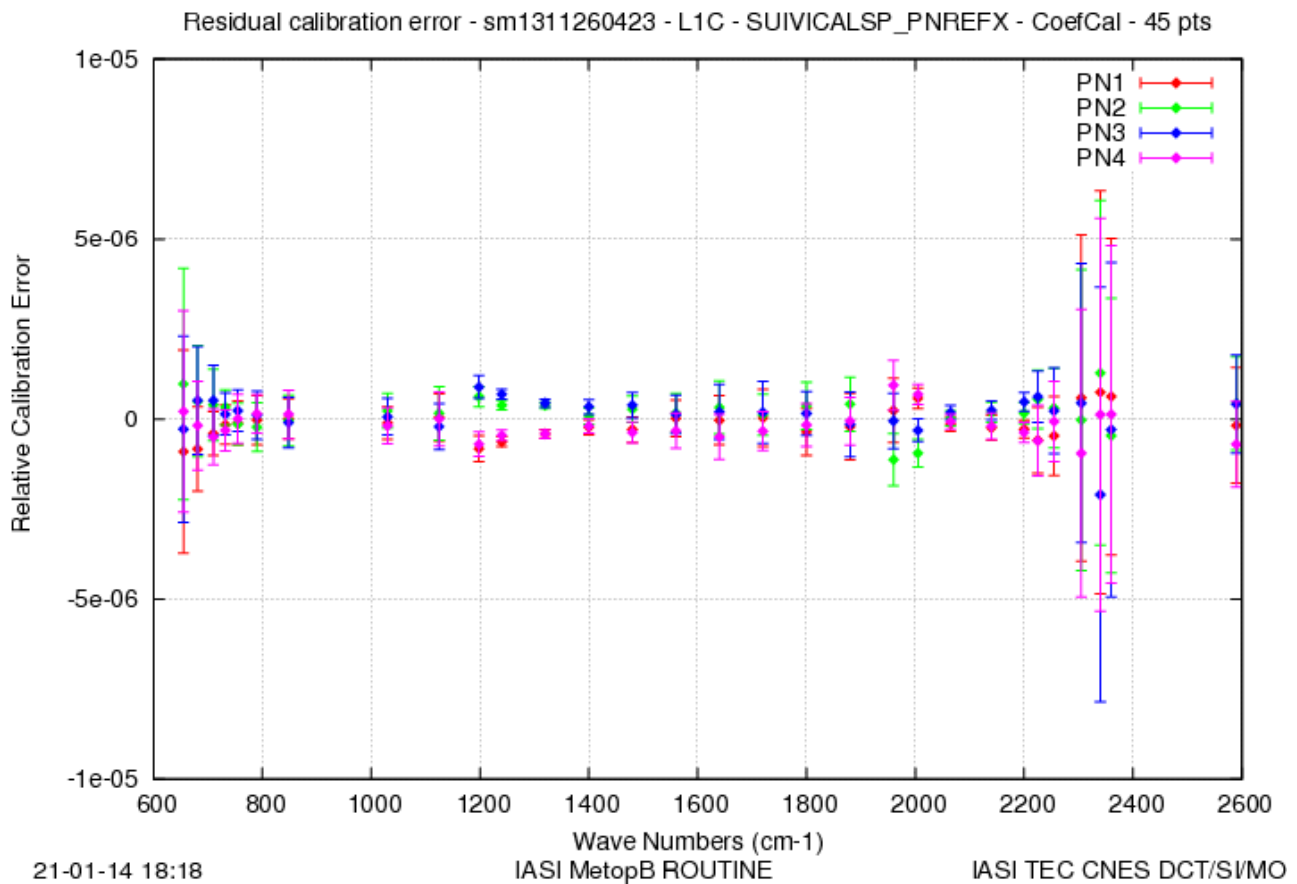


Figure 36 : Inter pixel spectral shift error for L1C IASI

The interpixel spectral calibration is better than 0.2ppm.

The results in the interband region are higher for the same reasons exposed in paragraph 4.6.2.1 . The error bars are high in B3 because of the noise that is higher at the end of B3.

In conclusion, the IASI pixels are spectrally independent.

4.6.3 Ghost evolution monitoring

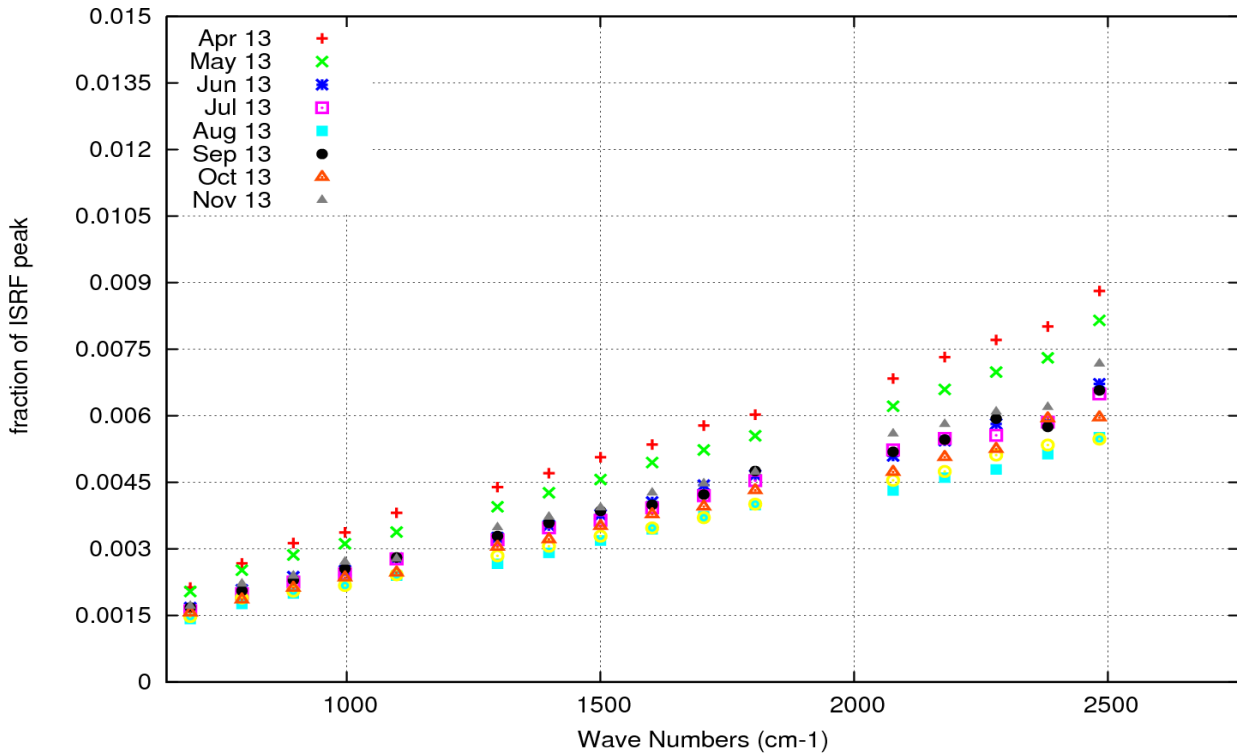
On-ground test of the instrument has shown a perturbation in the ISRF mainly caused by micro-vibrations of the interferometer separator blade. The amplitude of these micro-vibrations was characterized on ground and is measured on board.

Ghost origin is understood to be due to micro-vibrations of the beam-splitter. It is therefore stronger for the FOVs which project onto the top part of the beam-splitter (which vibrates more), and weaker for the FOVs which project onto the bottom part of the beam-splitter as it is attached to the optical bench.

The ghost affects the ISRF basically by replicating it at about $\pm 14\text{cm}^{-1}$. Of course, the amplitude of these replications is very low with respect to ISRF maximum value. The amplitude and the central wave number of ISRF replications are function of: cube corner velocity, frequency and mechanical amplitude of the beam-splitter vibration and wave number.

We are continuously monitoring the impact of the ghost on ISRF by monitoring, for each wave numbers, the maximum amplitude of the replicated ISRF with respect to ISRF_{max} value using monthly external calibration (BB views). The evolution over time of ghost amplitude with respect to ISRF_{max} amplitude is shown below for pixel 2 and 4.

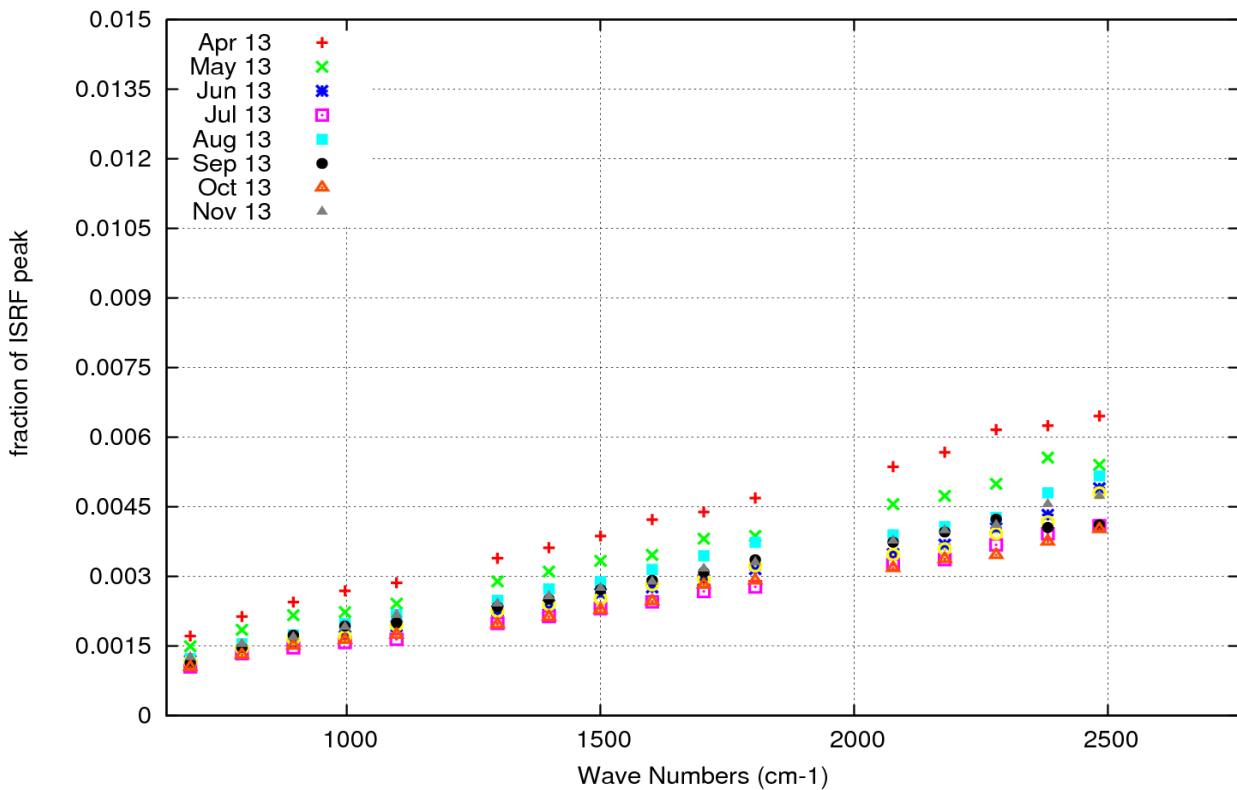
Ghost Amplitude Evolution (Max) - PN2



11-03-14 14:18 IASI PFM-R ROUTINE

CNES DCT/SI/MO

Ghost Amplitude Evolution (Max) - PN4





11-03-14 14:18 IASI PFM-R ROUTINE

CNES DCT/SI/MO

Figure 37 : Ghost amplitude as a function of wave number for different time (Top: pixel 2, bottom: pixel 4)

Maximum values of $ISRF_{max}$ (@2760 cm^{-1}) are respectively 0.9% for pixel 1-2 and 0.6% for pixel 3-4. We don't see any significant evolution over time.

		Doc n°: IA-RP-2000-4122-CNE Issue: 1.0 Date: 2017-09-27 Sheet: 52 Of: 60
--	--	---

Pseudo-noise induced by the ghost is lower than the 0.066K allocated specification and under control as soon as all cube corner velocity, frequency and mechanical amplitude of the beam-splitter vibration remain stable.

4.6.4 Conclusion

All parameters impacting IASI spectral calibration are stable and within specifications.

IASI has a fully satisfactory spectral calibration. The L1B processing, consisting in the spectral shift correction, and the L1C processing, consisting in the ISRF removal, are working very well.

4.7 GEOMETRIC PERFORMANCES

The geometric calibration is performed on ground (level 1 processing). Most of the analyses of geometric performances require being in external calibration mode.

Specifications are the following: the IIS/AVHRR co-registration has to be better than 0.3AVHRR pixel while the IIS/sounder co-registration has to be better than 0.8mrad.

4.7.1 Sounder / IIS co-registration monitoring

This monitoring is performed one time a year, generally around September for REVEX and march for mid-REVEX.

The sonder/IIS coregistration error is lower than 100μrad (eq. 100m on ground).

4.7.2 IIS / AVHRR co-registration

The IIS/AVHRR co-registration is permanently estimated by the L1 processing chain.

Note that AVHRR channels 4 and 5 are within the IIS spectral filter. The spatial resolution of the IIS (0,7km) is close to AVHRR (1km).

The IIS/AVHRR offset guess in the ground segment configuration is used when the algorithm of correlation between IIS and AVHRR does not converge (typically over homogeneous scenes).

The following figures show a comparison of IIS-AVHRR offsets (GIacOffsetIISAvhrr) mean profiles.

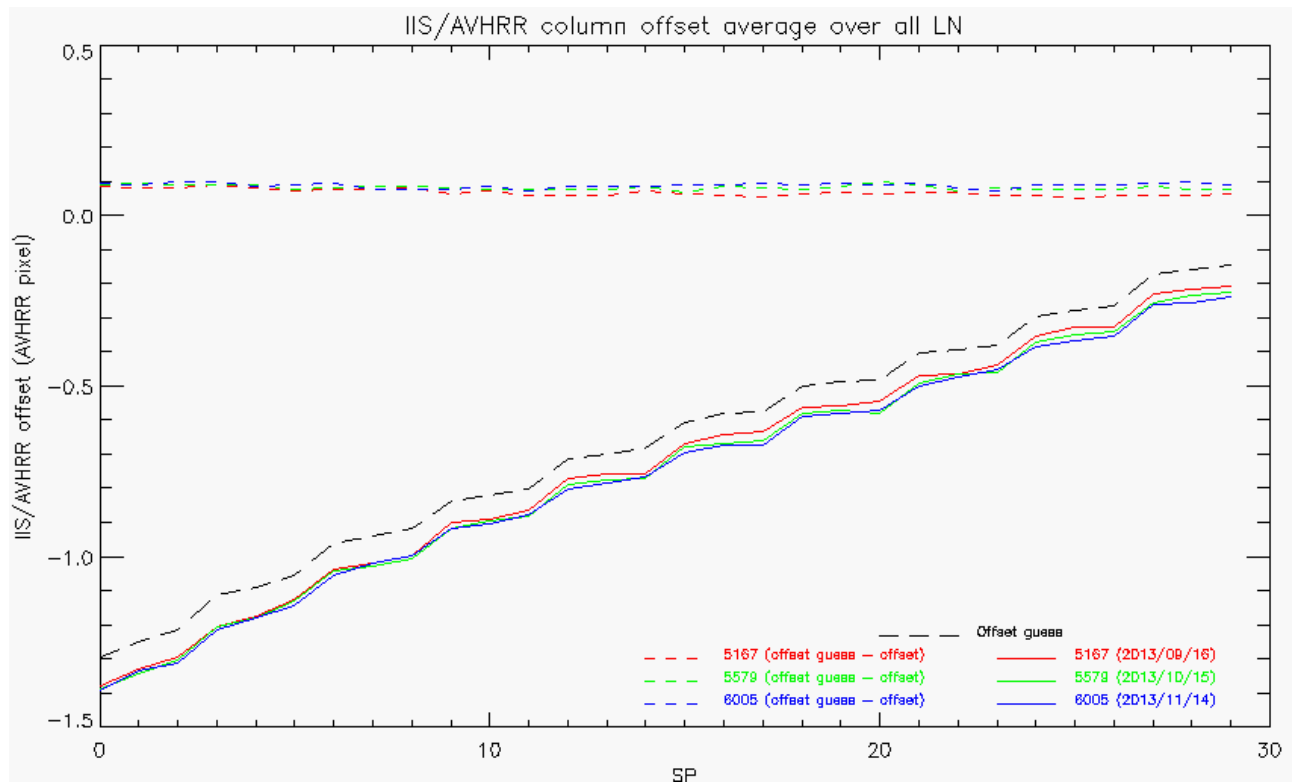


Figure 38 : Column offset (black) guess vs. column offset averaged over all lines (LN) as a function of the scan position (SP=SN), and orbit number

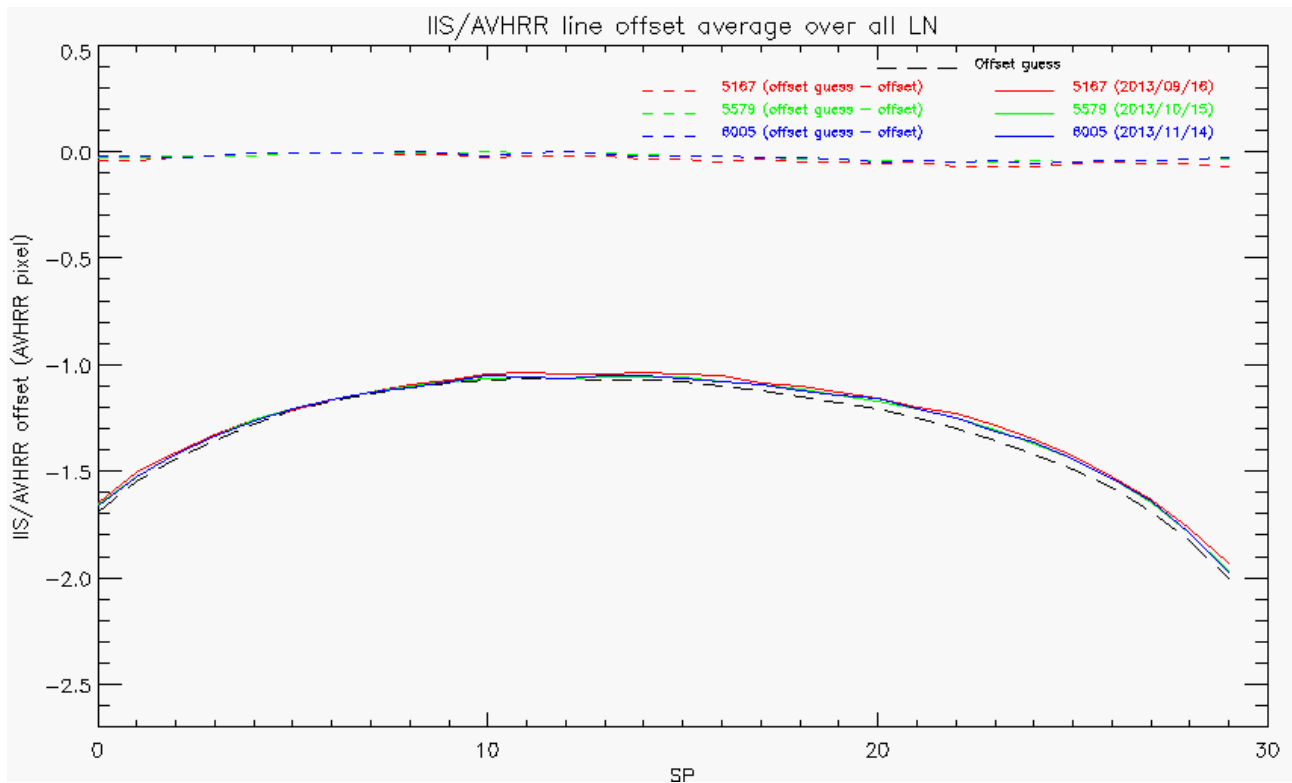


Figure 39 : Line offset guess (black) vs. line offset averaged over all lines (LN) as a function of the scan position (SP=SN), and the orbit number

For both across track and along track, the residuals between measured and IIS/AVHRR offset guess in the ground segment configuration are lower than 0.1 AVHRR pixel for all viewing angles, that is equivalent to 100m on ground.

The values are stable.

4.7.3 Conclusion

The positions of IASI pixel are considered stable and well within specification.

IIS-sounder co-registration is stable at about 100 μ rad which is equivalent to 100m on ground (specification : < 0.8 mrad).

IIS-AVHRR offset is lower than two pixels and stable over time: less than 0.1 AVHRR pixels over three months (specification: < 0.3 AVHRR pixel).

IASI pixel centre location accuracy in AVHRR raster is around 200m. The geolocation of IASI pixels are thus considered stable and well within specification (5 km).

4.8 IIS RADIOMETRIC PERFORMANCES

The main task of IIS is to insure a good relative positioning of IASI sounder pixels with respect to AVHRR. Its performances are studied each month using routine External Calibration data.

4.8.1 IIS Radiometric Noise Monitoring

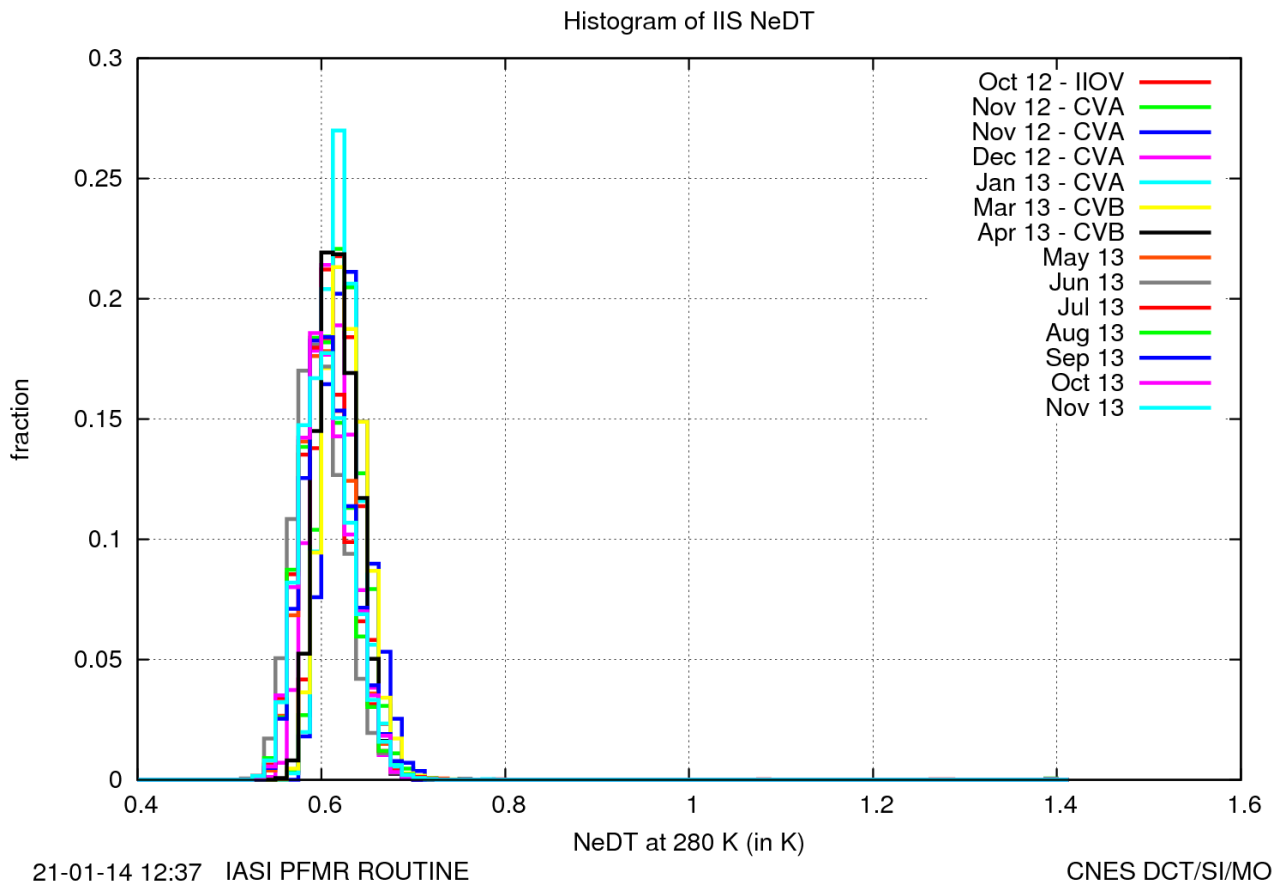




Figure 40 : Temporal evolution of the noise between start and end of the period

Radiometric noise of the IIS is very stable and lower than the specification of 0.8K.

		Doc n°: IA-RP-2000-4122-CNE Issue: 1.0 Date: 2017-09-27 Sheet: 56 Of: 60
--	---	---

4.8.2 IIS Radiometric Calibration Monitoring

In order to assess the stability of IIS radiometric calibration, we follow the time evolution of slope and offset coefficients. Figure 41 shows a comparison of slope and offset coefficients matrix between start and end of the period.

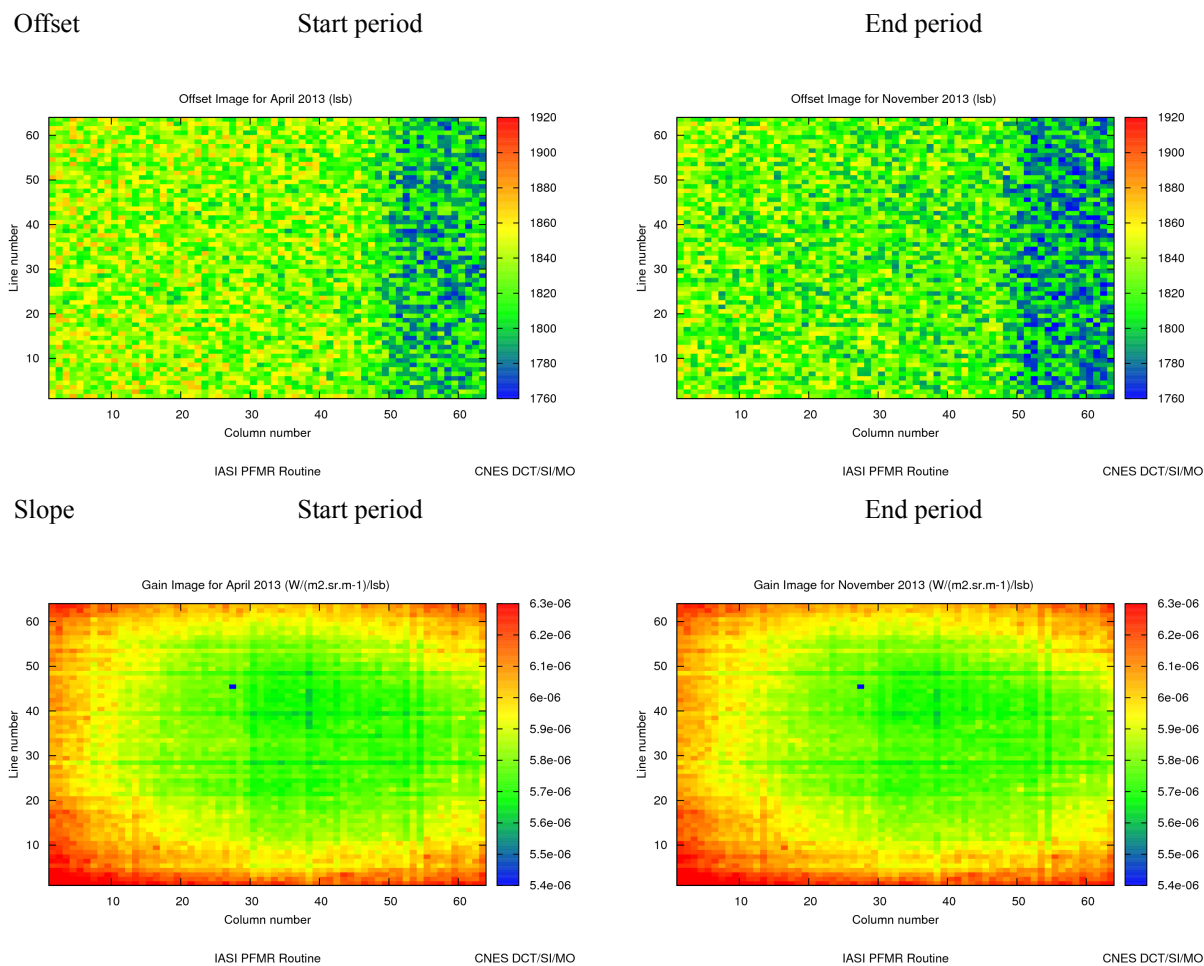
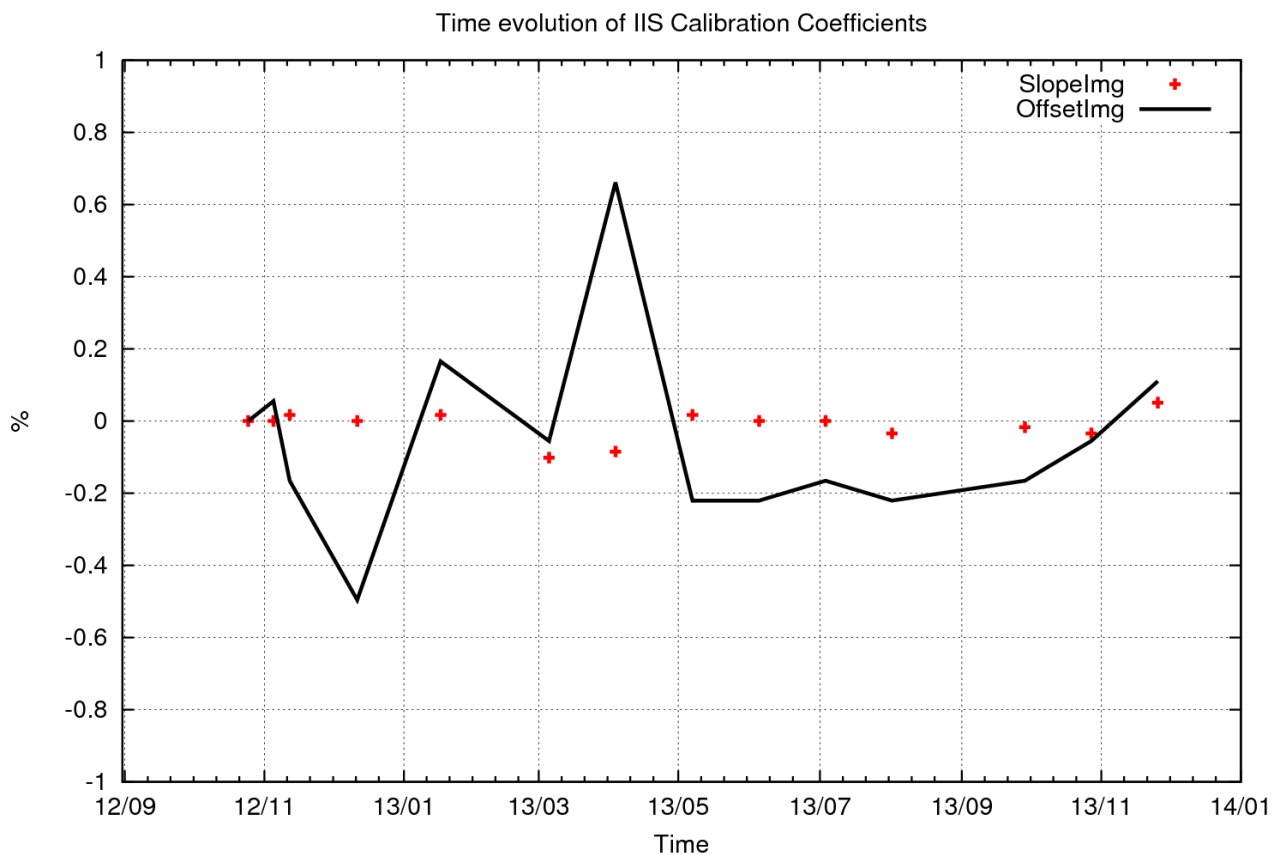


Figure 41 : Slope and offset coefficients matrix

The complete time series of average slope and offset coefficients is given in Figure 42.



21-01-14 12:37 IASI PFMR ROUTINE

CNES DCT/SI/MO

Figure 42 : Relative evolution in % of average of slope (red curve) and offset (black curve) coefficients

The slope coefficient is stable. Small variations of the offset coefficient are observed (between -0.5% and +0.7%).

The performances are nominal.

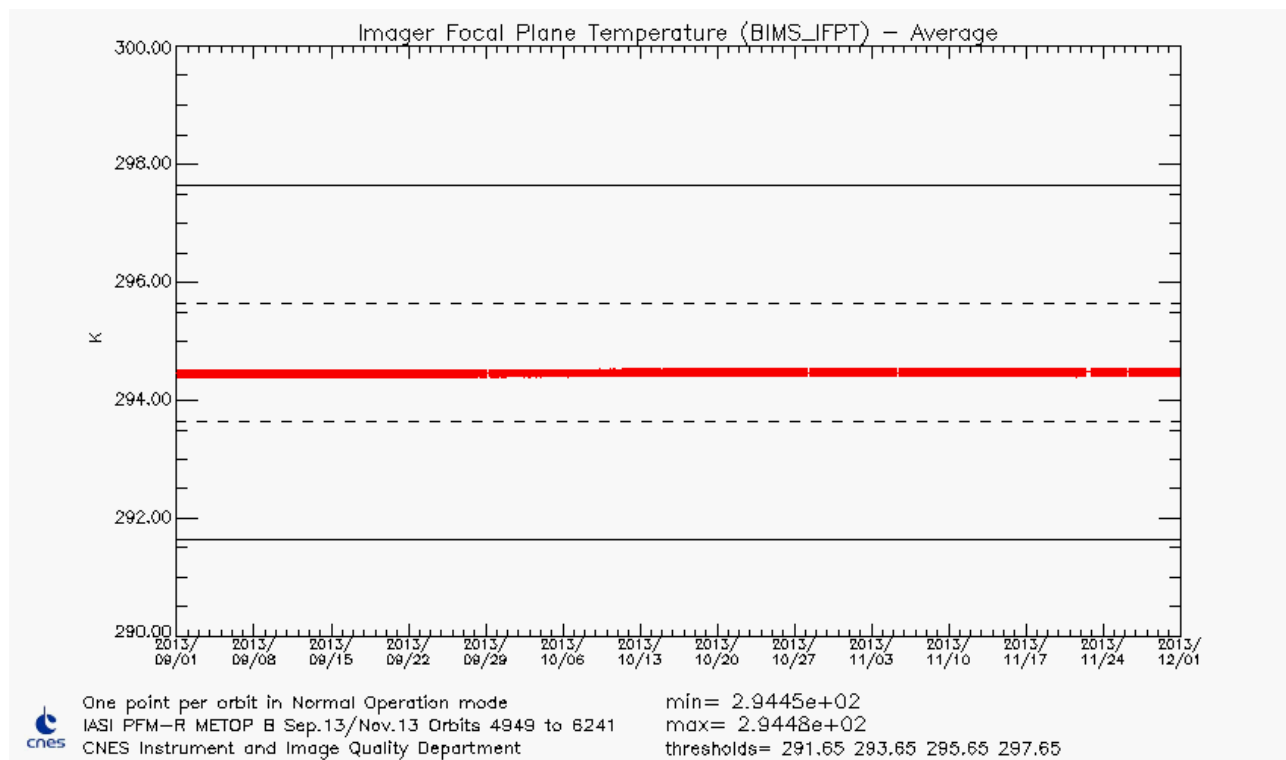




Figure 43 : IIS Focal Plane Temperature

4.8.3 Conclusion

The radiometric performance of IIS is very stable and within specification.

		Doc n°: IA-RP-2000-4122-CNE Issue: 1.0 Date: 2017-09-27 Sheet: 59 Of: 60
--	---	---

5 IASI TEC SOFTWARE AND INTERFACES

5.1 *IASI TEC EVOLUTION*

No evolution within the period.

Table 19 lists previous software evolutions.

IASI TEC software version	implementation	Comments
8.1	06 October 2011	Automatic downloads of L0 products from EUMETSAT FTP
8.2	12 April 2012	New version of product browser (handling IASI L0, L1C products and board configuration).
8.3	22 August 2012	Regularization version before IASI-B CAL/VAL CCAT replaced by CBST in TEC's logs

Table 19: IASI TEC at CNES Toulouse

5.2 *EUMETCAST INTERFACE*

EUMETCast dissemination is used for Near Real Time data reception by IASI TEC at CNES, Toulouse. Each orbit, L1 ENG, L1 VER, and AVHRR 1B products are received under continuous series of 3 minutes PDU. Full dumps are reconstructed by the EUMETCAST terminal and pushed to a IASI TEC server. Since August 2012, NPP/CrIS PDU are also received to perform inter-comparison with IASI.

In case of failure of the prime EUMETCAST station, products remain available several days on a redundant station.

The behaviour of the EUMETCAST reception is nominal.

The following table lists the recent modifications in the EUMETCAST configuration:



Date	EUMETCAST configuration
29/03/2011	End of IASI L0 dissemination via EUMETCAST
03/08/2011	Hardware and software upgrade of the prime station
04/12/2011	Hardware and software upgrade of the back-up station
13/07/2012	Software patch to correct an anomaly concerning AVHRR files (reception of 0 byte files from EUMETCAST)
24/08/2012	Modification of EUMETCAST configuration to receive NPP/CrIS data
03/2013	"PARALLEL_RECONSTRUCTIONS" set to 3 to avoid missing PDU problems
09/2013	"RECONSTRUCTION TIME-OUT" set to 90 to avoid missing PDU problems

Table 7-44 : EUMETCAST configuration at CNES Toulouse

5.3 *FTP INTERFACE*

Since March 29th of 2011, IASI L0 full dumps are available in Near Real Time on a EUMETSAT FTP server. The IASI TEC software automatically downloads products from the EUMETSAT FTP server.

The reception of L0 products at IASI TEC is nominal.

		Doc n°: IA-RP-2000-4122-CNE Issue: 1.0 Date: 2017-09-27 Sheet: 60 Of: 60
--	--	---

6 **CONCLUSION AND OPERATIONS FORESEEN**

Please visit <http://smsc.cnes.fr/IASI/> to get IASI news.

6.1 ***SUMMARY***

The IASI PFM-R instrument is fully operational.

The instrument configuration is the nominal one.

The main events are :

- IIS Equalization on 16 October 2013
- Out of Plane METOP manoeuvre on 5 November 2013
- Configuration PTSI 10 – NRD 37, GRD 18, ODB 12 and update of reduced spectra in November 2013
- Moon avoidance on November 22nd

6.2 ***SHORT-TERM EVENTS***

Moon on 21 December 2013

6.3 ***OPERATIONS FORESEEN***

- Next decontamination scheduled in March 2014.
- Update of scan mirror reflectivity mid 2014.

End of document